JOURNAL OF GEOPHYSICAL RESEARCH, VOL. 93, NO. A9, PAGES 9867–9882, SEPTEMBER 1, 1988

The Auroral 6300 Å Emission: Observations and Modeling

STANLEY C. SOLOMON[1], PAUL B. HAYS, AND VINCENT J. ABREU

Space Physics Research Laboratory, University of Michigan, Ann Arbor

Measurements of the auroral atomic oxygen (^3P–^1D) emission line at 6300 Å made by the Atmosphere Explorer visible airglow experiment are analyzed using a tomographic inversion. Emission altitude profiles are compared to the results from an electron transport and chemical reaction model. The model incorporates measurements of the energetic electron flux, neutral composition, ion composition, and electron density. Reasonable correspondence is obtained using primarily the "classical" sources of $O(^1D)$ excitation: electron impact on atomic oxygen and dissociative recombination of O_2^+. The reaction of $N(^2D)$ with O_2 is considered to be a minor source. Small contributions are also calculated for cascade from $O(^1S)$, electron impact dissociation of O_2, reaction of N^+ with O_2, and energy transfer from $O^+(^2D)$ and thermal electrons to $O(^3P)$. A possible minor source from the quenching of $N(^2D)$ or $N(^2P)$ by $O(^3P)$ is also discussed.

Introduction

The 6300 Å "red line" of atomic oxygen has been a particular problem for auroral studies. Although the transition which causes it is well known, there is little agreement on mechanisms resulting in the excited $O(^1D)$. Because of its low excitation energy and long radiative lifetime, it has a complex chemistry that is difficult to understand in the thermosphere and difficult to measure in the laboratory. Yet the most controversial point in the debate over the auroral sources is the degree to which the most straightforward process, impact of low-energy electrons on atomic oxygen, is responsible for the observed emission. If this source cannot account for most of the production rate, then some other must; the most notable candidate being the reaction of $N(^2D)$ with O_2.

Early studies of the atmospheric excitation of the $O(^1D)$ metastable have been reviewed by *Chamberlain* [1961], *Bates* [1978, 1982], and *Torr and Torr* [1982]. Studies by *Zipf and Fastie* [1963], *Dalgarno and Walker* [1964], *Fournier and Nagy* [1965], *Hunten and McElroy* [1966], and *Wallace and McElroy* [1966] examined the important mechanisms for production and loss of $O(^1D)$ in the upper atmosphere: photodissociation of O_2, impact of fast electrons on atomic oxygen, dissociative recombination of O_2^+ (which was first proposed by *Bates* [1946] as a nightglow source), quenching by N_2 and O_2, and spontaneous emission. Quantification of these reactions has been accomplished over the last two decades by a combination of satellite, rocket, ground based, and laboratory experiments and theoretical studies; notably *Rees et al.* [1967], *Henry et al.* [1969], *Nagy and Banks* [1970], *Noxon and Johanson* [1970], *Zipf* [1970], *Dalgarno and Lejeune* [1971], *Hernandez* [1972], *Brown and Steiger* [1972], *Walls and Dunn* [1974], *Sharp et al.* [1975], *Rees and Roble* [1975], *Rusch et al.* [1975], *Kernahan and Pang* [1975], *Streit et al.* [1976], *Hays et al.* [1978], *Mul and McGowan* [1979], *Cogger et al.* [1980], *Torr and Torr* [1981], *Link et al.* [1981], *Abreu et al.* [1983], *Shyn and Sharp* [1986].

A key parameter is the total Einstein probability for the $O(^3P$–$^1D)$ radiative transition. The estimate by *Garstang* [1951, 1956] of $A_{1_D}=9.1\times10^{-3}$ s^{-1} (where $A_{1_D}=A_{6300}+A_{6364}+A_{6392}$) has been widely used in aeronomic studies despite his later revision [*Garstang*, 1968] to 6.7×10^{-3}. The *Kernahan and Pang* [1975] laboratory measurement of $(6.8\pm1.3)\times10^{-3}$ is close to the revised value but *Fischer and Saha* [1983] calculated a value of 9.4×10^{-3}. There is agreement, however, that $A_{6300}/A_{1_D}=0.76$. Attempts to use thermospheric nightglow measurements [*Hays et al.*, 1978; *Abreu et al.*, 1983] to establish the yield of $O(^1D)$ from dissociative recombination of O_2^+ and its rate of quenching by N_2 are sensitive to the choice of Einstein coefficients [*Link et al.*, 1981]. The question is further complicated by the possibility that $O(^3P)$ plays a role in quenching [*Yee et al.*, 1988]. *Abreu et al.* [1986] found that this is a significant loss mechanism for $O(^1D)$, although not the major loss channel; *Link and Cogger* [1988] did not agree.

Turning now to the auroral 6300 Å emission, *Rees et al.* [1967] proposed that $O(^1D)$ is produced in auroræ by impact of secondary auroral electrons and thermal electrons on atomic oxygen, dissociative recombination of O_2^+, and cascade from $O(^1S)$:

$$e^* + O(^3P) \rightarrow e^* + O(^1D) \quad (1)$$

$$e_t + O(^3P) \rightarrow e_t + O(^1D) \quad (2)$$

$$O_2^+ + e \rightarrow O + O(^1D) \quad (3)$$

$$O(^1S) \rightarrow O(^1D) + h\nu_{\lambda=5577\,\text{Å}} \quad (4)$$

These conclusions were not seriously altered for a decade [cf. *Rees and Jones*, 1973; *Rees and Luckey*, 1974]. Process (1) has been considered to be the largest source, and although only theoretical estimates of the cross section of atomic oxygen for production of $O(^1D)$ from electron impact were available for some time, recent measurements [*Shyn and Sharp*, 1986] are in general agreement with theory [*Henry et al.*, 1969; *Vo Ky Lan et al.*, 1972; *Thomas and Nesbet*, 1976]. *Gulcicek and Doering* [1986] and *Doering and Gulcicek* [1987] measured a cross section at that is smaller than that of Shyn and Sharp at 30 eV but larger at 20 eV; however, these results are still preliminary and do not yet extend to lower energies.

Analysis of auroral rocket measurements by *Sharp et al.* [1979] found that far more 6300 Å emission was observed than could be accounted for by (1)–(4), leading to the suggestion by *Rusch et al.* [1978] that the reaction

$$N(^2D) + O_2 \rightarrow NO + O(^1D, ^3P) \quad (5)$$

could account for the auroral red line if the yield of $O(^1D)$ were near unity. This was based on a laboratory study by *Kennealy et*

[1]Now at National Center for Atmospheric Research, Boulder, CO.

Paper number 7A9270.
0148–0227/88/007A–9270$05.00

al. [1978] in which the vibrational excitation of NO produced in this reaction was observed to have a structure consistent with an $O(^1D)$ yield of up to 0.8. Besides providing the additional source required by the rocket observation, the reaction would explain why the 6300/5200 Å emission ratio had been observed, up to that time, to be relatively constant in aurorae [*Gérard and Harang*, 1973], since $O(^1D)$ is destroyed mainly through quenching by N_2 and the N_2/O_2 density ratio exhibits slight variation in the 150–250 km region.

The *Kennealy et al.* [1978] experiment only placed an upper limit on production of $O(^1D)$ by (5), so evidence for the importance of this reaction is indirect, but this mechanism has been widely cited in reviews and adopted in thermospheric models [cf. *Bates*, 1982; *Torr and Torr*, 1982; *Roble et al.*, 1987]. *Torr et al.* [1980, 1981] calculated that (5) would be an important source of $O(^1D)$ in the dayglow, and *Rees et al.* [1983] adopted it for auroral calculations with a high yield of $O(^1D)$. However, the supposition concerning the constancy of the 6300/5200 Å emission ratio was not substantiated. *Link* [1982, 1983] and *Link et al.* [1983] presented measurements from a rocket flight in the dayside cleft and polar cap which found large variation in this ratio. Due to its long thermospheric lifetime, $N(^2D)$ can be transported out of the auroral oval and into the polar cap [*Gérard and Roble*, 1982]; elevated 5200 Å emission levels in this region were not accompanied by 6300 Å emission to any significant degree which is evidence against (5) as a source of $O(^1D)$. Variations in the overhead brightness ratio alone do not disprove the validity of the mechanism because $N(^2D)$ is lost through quenching by atomic oxygen and electrons as well as through reaction with O_2, particularly at higher altitudes where transport is more effective. But a chemical and dynamical model [*Link*, 1982] taking these processes into account was used to establish an upper limit for the yield of $O(^1D)$ from (5) of 0.2, later reduced to 0.1 [*Link*, 1983]. Ground based observations at high latitude [*Duboin et al.*, 1984] confirmed the 6300/5200 Å variations in the polar cap, and *McDade and Llewellyn* [1985] also found support for a low yield in a rocket study of auroral O_2 atmospheric band emission. Nevertheless, the discrepancy between observed 6300 Å emission and calculated $O(^1D)$ densities (in the absence of (5)) was also found by *Sharp et al.* [1983] using data from the AE–D satellite. *Rees and Roble* [1986] also considered (5) to be the major source of auroral $O(^1D)$.

Although the definitive laboratory study which could resolve the question of the yield of $O(^1D)$ from (5) has not been done, there has been one important experiment. *Langford et al.* [1985, 1986] measured the yields of excited states of atomic oxygen produced by

$$N^+ + O_2 \rightarrow NO^+ + O \quad (6a)$$

$$N^+ + O_2 \rightarrow O_2^+ + N \quad (6b)$$

$$N^+ + O_2 \rightarrow NO + O^+ \quad (6c)$$

which is a minor source of $O(^1D)$ in the aurora (yield=0.7±0.3). $N(^2D)$ is produced by (6*b*) but the possibility that (5) contributed substantially to the experimental production of $O(^1D)$ was ruled out by the observed absence of any molecular oxygen pressure dependence of the monitored emission, since (5) is 100 times slower than (6). Langford et al. therefore support the *Link* [1983] estimate of a yield of $O(^1D)$ from (5) less than 0.1.

Weill [1969] suggested that quenching of $N(^2D)$ by atomic oxygen

$$N(^2D) + O(^3P) \rightarrow N(^4S) + O(^1D) \quad (7)$$

could be a significant source of $O(^1D)$ in the day and nightglow with even a small efficiency of production; the auroral abundance of $N(^2D)$ would imply that this is a non-negligible source in the aurora as well. However, theoretical studies of potential curves [*Black et al.*, 1969; *Olson and Smith*, 1974] indicate that the probability for production of $O(^1D)$ is less than 0.03 and so the process is not expected to be significant [*Torr and Torr*, 1982]. Other possible mechanisms for auroral production of $O(^1D)$ include energy transfer from excited atomic oxygen ions [*Mahadevan and Roach*, 1968]

$$O^+(^2D) + O(^3P) \rightarrow O^+(^4S) + O(^3P, {}^1D) \quad (8)$$

and electron impact dissociation of O_2

$$e^* + O_2 \rightarrow e^* + O(^3P) + O(^1D) \quad (9)$$

The yield of $O(^1D)$ from (8), if any, is not known but this is unlikely to be a significant source except possibly at very high altitudes because $O^+(^2D)$ reacts rapidly with N_2 [*Gérard*, 1970]. Process (9) is also minor due to the small cross section and low O_2 density. Schumann-Runge photodissociation of O_2 in the night aurora may be ruled out by virtue of the insufficient strength of auroral emissions in the 1350–1750 Å range, although this is of course an important dayside source of $O(^1D)$.

Thermal electron excitation of atomic oxygen (2) is a possible auroral source of $O(^1D)$, but elevated ambient electron temperature levels appear to be required to make this an important mechanism in the nightside aurora. Stable auroral red (SAR) arcs, which occur at lower latitude and higher altitude than the polar aurora, are an exception. This spectrally pure 6300 Å emission is caused by (2) [*Kozyra*, 1985] but is not truly an auroral phenomenon. High altitude cleft emission regions also may have a substantial contribution from (2), particularly when sunlit. The review of cleft auroral processes by *Shepherd* [1979] did not consider (2) to be an important source of $O(^1D)$ excitation compared to impact by low-energy electrons, but radar observations by *Wickwar and Kofman* [1984] of greatly elevated electron temperatures coincident with high altitude 6300 Å emission in the (dark) cleft region show that this is an important source under certain conditions. Electron temperatures above 2500 K are required to make this source significant, although once in this temperature range the rate coefficient increases rapidly. These temperatures are not usually reached in the nightside aurora.

Finally, the reactions of $N(^2P)$ may be considered:

$$N(^2P) + O_2 \rightarrow NO + O(^3P, {}^1D) \quad (10)$$

$$N(^2P) + O(^3P) \rightarrow N(^2D) + O(^3P) \quad (11a)$$

$$N(^2P) + O(^3P) \rightarrow N(^4S) + O(^3P, {}^1D) \quad (11b)$$

The auroral chemistry of $N(^2P)$ was investigated by *Zipf et al.* [1980]. Their conclusion that (11) is very efficient at reducing $N(^2P)$ to $N(^2D)$ or $N(^4S)$ means that auroral $N(^2P)$ densities will be much lower than $N(^2D)$, precluding (10) as a significant source of $O(^1D)$ regardless of the yield, which may be high [*Rawlins*, 1986]. The relative importance of (11*a*) versus (11*b*) is not known, although Zipf et al. speculate that (11*a*) dominates, and production of $O(^1D)$ is not energetically possible through this path. Even if (11*b*) is significant, it may produce little $O(^1D)$. Since $N(^2P)$ is too short lived to be transported it is not subject to the objections concerning the observed 6300/5200 Å variations. Furthermore, $N(^2P)$ is produced by electron impact on N_2 but not significantly by dissociative recombination of NO^+ so it should cause no additional difficulties for the nightglow.

MEASUREMENTS OF THE AURORAL 6300 Å EMISSION

Instrumentation for the Atmosphere Explorer mission is described in *Radio Science*, volume 8, number 4, 1973. The visible airglow experiment (VAE) [*Hays et al.*, 1973] consisted of a two-channel filter wheel photometer designed to monitor airglow and auroral emission features in the upper atmosphere. The channels were oriented perpendicular to one another such that when the satellite was spinning, the two photometers turned within the orbital plane. The channel one photometer had a 0.75° half angle cone field of view for high spatial resolution while channel two had a 3.0° half angle cone. Integration periods of 0.031 s for channel one and 0.125 s for channel two were matched to the spin rate of the satellite so that counts were summed over angular intervals roughly equal to the field of view when spinning. This resulted in sensitivity in the neighborhood of 20 R/count/integration for channel one and 0.3 R/count/integration for channel two. The filter wheel had six interference filters, a dark position, and a calibration position. Spectral resolution was from 15–30 Å. The laboratory calibration was estimated to have an absolute accuracy within 20%, and the signal-to-noise ratio is specified by Poisson statistics to be equal to the square root of the number of counts.

VAE limb brightness and nadir observations are interpreted using the tomographic inversion of *Solomon et al.* [1984, 1985]. The most complete description of this algorithm is in *Solomon* [1987]. Essentially, the method is to use many sets of limb scans to obtain the volume emission rate distribution of the emitting function by application of an equation derived by *Cormack* [1963]. This equation relates the Fourier transform of a function of two polar variables with respect to the angular variable to the Fourier transform of the function describing its line integrals. The inversion recovers a two-dimensional slice of the volume emission rate as a function of altitude and angle along the satellite track, enabling the recovery of the volume emission rate profile in each column below the satellite. During the night, the horizontal resolution of the inversion may be greatly increased by application of nadir data, or measurements taken while the photometer looked directly down at the emitting region, to the limb scan inversion. The influence of light scattered from clouds, lower atmosphere, and ground is removed following the method of *Hays and Anger* [1978].

As the $O(^1D)$ metastable is quenched by molecular nitrogen and other species, emission is mostly above 150 km and generally peaks in the 200–300 km region in the dayglow, nightglow, and aurora; the SAR arc, which usually occurs above 400 km, is an exception. This behavior is fortunate for interferometric study of the 6300 Å line shape to recover winds and temperatures as the altitude with which these properties may be associated remains fairly constant. The high, broad altitude profile associated with the auroral red line also renders it an attractive object for study with satellite photometry; several examples of VAE observations interpreted via the tomographic algorithm are presented here.

AE–C orbit 4389 was nearly circular, with satellite altitude over 400 km in the auroral zone. Inversion of the auroral segment the using VAE channel one with nadir data included is shown in Figure 1*a*. The albedo was estimated to have a value of 0.8 by comparing the inverted limb brightness measurements to the nadir vertical column brightness function [*Solomon et al.*, 1985]. This is a reasonable albedo for the combination of clouds, ice, and snow expected to be below the satellite during a winter auroral pass. There is a small feature at high dip latitude

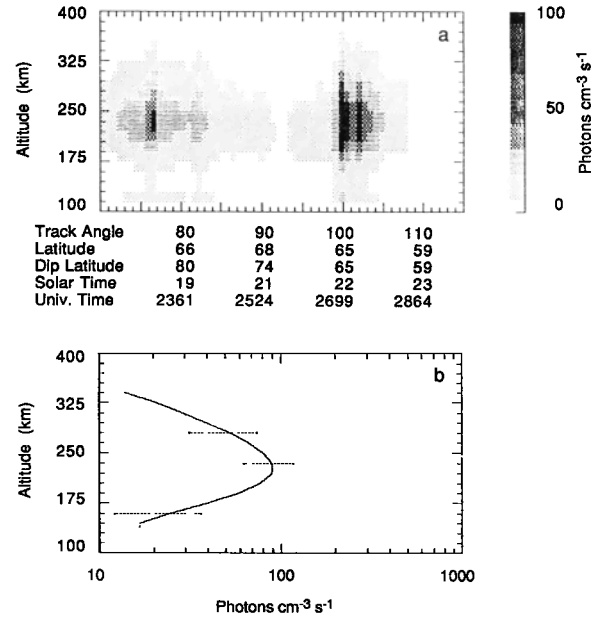

Fig. 1. (*a*) Auroral 6300 Å emission from inversion of AE–C orbit 4389. (*b*) Altitude profile of the brightest column from AE–C orbit 4389, with estimated error bars.

near the terminator and another, brighter, aurora at 65° dip latitude. The volume emission rate altitude profile of the brightest inversion column is plotted in Figure1*b*. The emission increases with decreasing altitude at a scale height of about 40 km in the high altitude region where quenching is unimportant, reaches a peak near 220 km, and rapidly decreases below there as quenching sets in.

Figures 2*a* and 2*b* show inversions of two auroral transits on a night when several occurred with full instrument function and the 6300 Å filter on VAE channel one. Satellite altitude was near 250 km throughout, and magnetic activity was low, $Kp = 1$ to 3. The altitude scale has been changed to 5 km resolution due to proximity to the peak emission region. Another northern hemisphere winter orbit, AE–C 5631, is displayed in Figure 2*c*. The satellite altitude is yet lower, near 245 km. Orbit 6136, shown in Figure 2*d*, passed over the aurora australis during southern hemisphere autumn. This orbit observed the brightest 6300 Å aurora found in the AE data base, with peak volume emission rate above 200 photons cm^{-3} s^{-1}. The slow decrease below the peak is associated with high mean electron energy of approximately 7.0 keV.

These observations of the auroral 6300 Å emission were made during a low solar activity regime—the $F_{10.7}$ index was below 100 throughout the period. Also, no major magnetic storms or extremely bright auroral events have been found with the necessary filter wheel position for 6300 Å measurements. Subtle changes with electron flux characteristics are present, though, and these may be exploited to analyze the magnitude of proposed $O(^1D)$ source and sink mechanisms.

OBSERVATIONS OF THE ENERGETIC ELECTRON FLUX

The principal instrument used in this study for measurement of energetic electron fluxes in the aurora is the low-energy electron experiment (LEE) carried by the AE–C and AE–D satellites. This instrument is described by *Hoffman et al.* [1973]. The stepped-energy electron detector on AE–C was chosen to

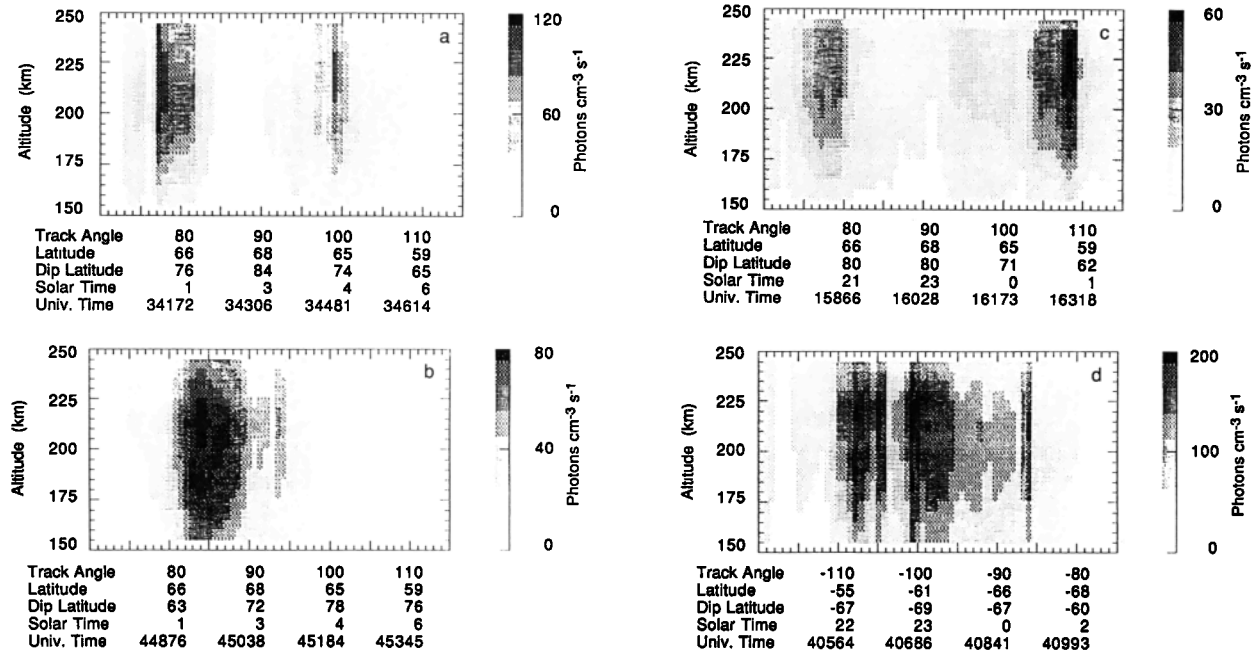

Fig. 2. Auroral 6300 Å emission from inversion of four orbits. (*a*) AE–C orbit 5376. (*b*) AE–C orbit 5378. (*c*) AE–C orbit 5631. (*d*) AE–C orbit 6136.

be the main source of flux measurements for comparison with photometric observations. The time for one complete energy cycle from 0.2 to 26 keV was one second; this corresponds to approximately 8 km of distance along the satellite track and it is possible to miss important parts of a structured event using a single detector in this fashion. This time span is small, however, compared to the 15 s spin period of the satellite. The 5 keV detector measurements were examined to determine whether such structure was a problem for any of the auroral events, and the stepped proton detector was used to assure that precipitating protons did not play a significant role, as they were not included in the model.

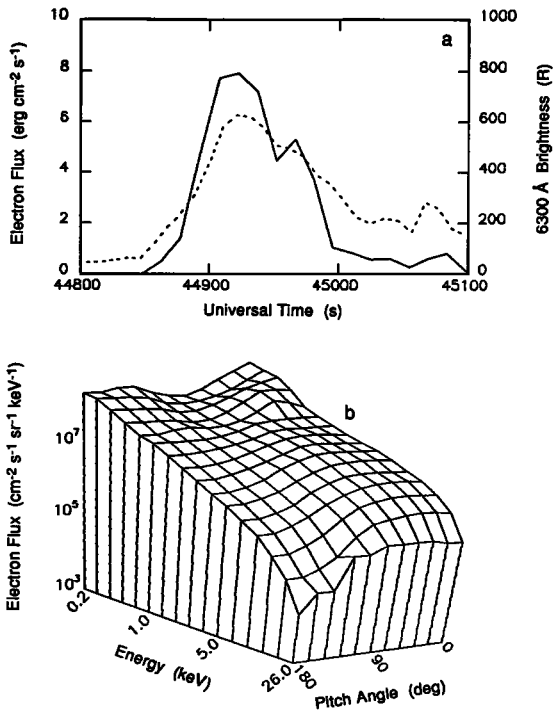

Fig. 3. Auroral electron flux from AE–C orbit 5378 measured by the LEE instrument. (*a*) Total energy flux over the range 0.2–26 keV (solid line) with 6300 Å vertical column brightness integrated from 150–245 km (dotted line) over-plotted for comparison. (*b*) Dependence on energy and pitch angle of the differential number flux averaged over the interval from 44890 to 44990 s UT.

The angle between the field line and an electron velocity vector is defined as the pitch angle ξ; the flux in any direction $\varphi(E,\xi,\psi)$ in electrons cm^{-2} s^{-1} sr^{-1} eV^{-1} is then a function of energy, pitch angle and azimuthal angle ψ. The distribution of flux is not expected to depend on ψ, but it does vary with ξ; this is measured by the spinning satellite as the detector scans different angles to the magnetic field. Hemispherical fluxes $\Phi_d(E)$ $\Phi_u(E)$ are defined for the downward and upward directions as the integral over a hemisphere of the component of the flux along the field line. The total downward (or upward) energy flux, is then defined as the integral over energy of the respective hemispherical flux, given in erg cm^{-2} s^{-1}. Figures 3 and 4 display the downward energy fluxes during two of the AE–C orbits for which inverted 6300 Å auroral emission data was shown above; the vertical column brightness obtained by integrating from the satellite altitude to the lowest inversion level is also plotted for morphological comparison. (This column brightness is less than the total brightness that would be observed from the ground, as it does not include any emission above the satellite orbit or at low altitude.) The ratio between energy and brightness is not constant as changing flux characteristics and atmospheric composition cause varying amounts of O(^1D) excitation. The curve shapes correspond quite well, although the locations of peaks are sometimes displaced by about 10 s. This is partially due to the angular offset between photometer and electron detector of 135°, a small portion may be due to the angle of the magnetic field. Also displayed with these figures is a surface plot of the dependence of the electron flux on energy and pitch angle averaged over a section of each orbit corresponding to an auroral precipitation event. Examination of

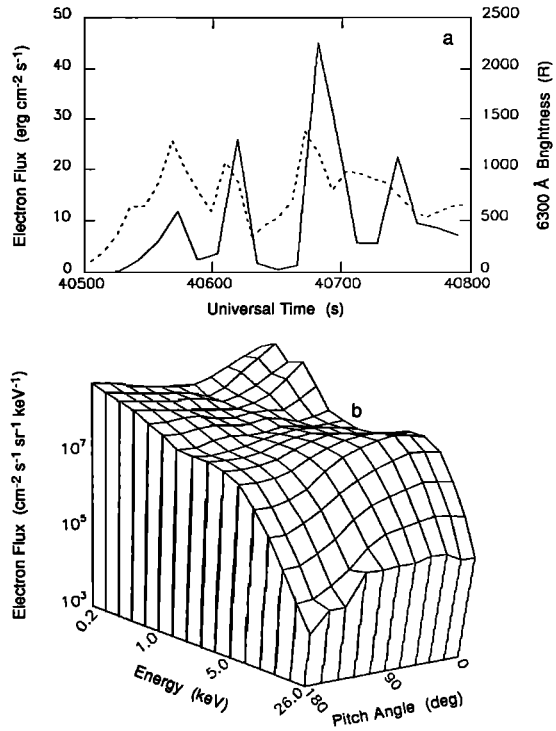

Fig. 4. Auroral electron flux from AE–C orbit 6136 measured by the LEE instrument. (*a*) Total energy flux over the range 0.2–26 keV (solid line) with 6300 Å vertical column brightness integrated from 150–245 km (dotted line) over-plotted for comparison. (*b*) Dependence on energy and pitch angle of the differential number flux averaged over the interval from 40650 to 40740 seconds UT.

these figures reveals that for these events, at these altitudes, downward hemispherical isotropy is a good approximation.

The energy range of the detector was sufficient to characterize the primary flux, although some electrons had higher energies than those measured; see Figure 4 where a fairly hard flux from AE–C orbit 6136 is shown. Considering the logarithmic scale, however, the portion of the flux with energy greater than the maximum measured is not significant. Protons were also monitored for these orbits but are not plotted because the fluxes were extremely low. There is always the possibility of high energy proton events undetectable by the instrument but these would cause spikes in the 4278 Å emission which was monitored in the nadir direction on VAE channel two, and were not observed.

The photo-electron spectrometer (PES) [*Doering et al.*, 1973] measured electron fluxes in the interval 2–500 eV, overlapping with the LEE detectors in the upper portion of its range. This provides a check on the accuracy of measurements from 200–500 eV, and should yield the secondary electron spectrum as well. However, interpretation of auroral PES data is difficult, particularly at low energy. One problem is that the energy band pass of the instrument was a constant fraction of electron energy detection level so sensitivity decreased with energy; this resulted in very low count rates for energies less than about 50 eV when the instrument was in high spatial resolution mode. Another difficulty is the spacecraft shadowing effect; at certain orientations the spiral trajectories of the electrons are blocked from entering the detector by the body of the satellite itself. Also, ram and wake effects modulate low energy measurements at twice the satellite spin frequency. In addition there is the question of the effect of spacecraft charging and magnetization, which could degrade the instrument's sensitivity and interfere with electron detection.

Nevertheless, two attempts to utilize these measurements are shown here. The first, which is plotted in Figure 5*a*, uses PES summary data from the unified abstract (UA) files for the only orbit for which both auroral 6300 Å and PES UA data are available, AE–C 5376. The electron spectrometer was in a variable sweep interval mode rather than the high spatial resolution mode, and the summary data specify the differential energy flux of electrons at 6 points, averaged over pitch angle (the fluxes are reasonably isotropic at low energies.) These are compared with LEE measurements near the region of energy overlap. Both measurements were averaged over the same 90 s interval. The comparison is fair in the overlap region but at low energy the collisional transport model employed (see below) shows a much faster rise of the secondary flux with decreasing energy than the PES measurements. Another approach is to average over a discrete precipitation event while the instrument was in high spatial resolution mode and compare with similarly averaged LEE measurements. This was done for a single intense event on AE-C orbit 6136, and the result plotted in Figure 5*b*. The comparison is again reasonable but the rate at which the PES flux increases with decreasing energy is still less than expected.

This question of secondary electron energy dependence has been controversial for some time and is in fact at the heart of the $O(^1D)$ electron impact excitation rate debate. It is generally agreed that primary fluxes in the 1–20 keV range produce a secondary flux whose spectral shape in the 10–100 eV interval is described by a power law, i.e., the differential flux is proportional to $E^{-\gamma}$ where γ is the spectral index. On the one hand are laboratory experiments [*Opal et al.*, 1971] and collisional

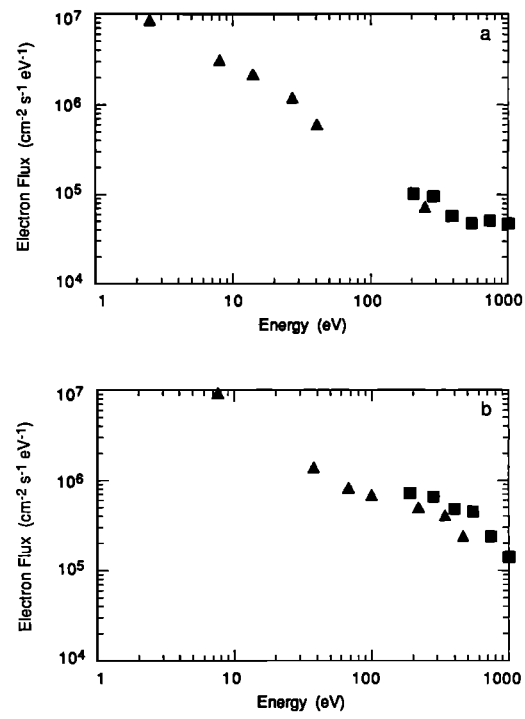

Fig. 5. Low-energy hemispherical electron fluxes measured by PES (triangles) and LEE (squares). (*a*) AE–C orbit 5376. Fluxes from the UA data base averaged over the interval from 34100 to 34190 UT. (*b*) AE–C orbit 6136. Fluxes integrated over a half-spin of the satellite (0°–180° pitch angle) from 40702 to 40709 UT.

models [e.g., *Banks et al.*, 1974; *Evans*, 1974; *Strickland et al.*, 1976; *Stamnes*, 1981] which support γ~2 with little dependence on the primary characteristic energy. On the other hand are collisionless models [*Papadopoulos and Coffey*, 1974; *Stasiewicz*, 1984] which support certain atmospheric measurements of γ~1 [e.g., *Sharp and Hays*, 1974; *Doering et al.*, 1976, and other PES spectra such as those shown here]. Of course, the situation is never so simple as to allow the straightforward fit of data by a single parameter; for instance, *Sharp et al.* [1979] measured spectra characterized by γ~2 in the 10–100 eV interval at 143 km, decreasing to γ~1 as the rocket ascended to 245 km. If the typical spectral index at 100–300 km altitude is substantially less than 2.0, a great deal of this work would be invalidated as there would be far fewer low-energy electrons produced. But recent measurements from the low altitude plasma instrument (LAPI) on Dynamics Explorer 2 [*Fung and Hoffman*, 1988] agree with some older ones [*Frank and Ackerson*, 1971; *Reasoner and Chappell*, 1973] that a value of γ~2 is appropriate for "inverted-V" auroral fluxes. The LAPI results found γ to decrease slowly with increasing altitude from 2.0 at 325 km to 1.7 at 950 km; the overall average was γ=1.85. There was little systematic variation with pitch angle but there was a negative correlation with the peak energy of the primary beam. Extrapolation from the lower limit of the altitude range at 325 km down to 250 km yields γ~2.2, which happens to be the value predicted by the Banks and Nagy two-stream model adopted here. For these reasons, AE–C PES auroral measurements are not used in this work. This is a matter of some concern as the central conclusions obtained herein hinge on the question of correct determination of secondary electron fluxes.

Model of the Auroral 6300 Å Emission

The electron transport algorithm selected for analysis of LEE particle flux measurements is the model developed by *Banks and Nagy* [1970], *Nagy and Banks* [1970], *Banks et al.* [1974] which is generally referred to as the Banks and Nagy two-stream code. This method was originally developed for photoelectrons and later extended to higher electron energies for auroral computations. The electron flux is calculated using the two-stream approximation to the transport equations, solving for the upward and downward hemispherical fluxes along a magnetic field line as a function of energy. The effects of gravity, parallel electric fields, and magnetic field convergence are neglected. Elastic collisions with three neutral species (O, N_2, O_2), discrete energy losses from inelastic collisions resulting in excitation and ionization of these species, and thermal excitation of the ambient electron gas are considered. Electron impact cross sections and backscatter ratios used in the model are described in Appendix A. Thermalization of fast electrons by the ambient electron gas was treated as in *Swartz et al.* [1971]; [cf. *Schunk and Hays*, 1971]. A continuously variable energy grid was employed with 190 bins from 0.25 eV to 49.0 keV, and a method similar to that of *Swartz* [1985] adopted for energy redistribution. Because the model does not consider pitch angle variation, it is necessary to assume an average cosine of the pitch angle which appropriately characterizes the transport; the value μ=0.577 was used here as recommended by *Banks et al.* [1974].

Hemispherical fluxes $\Phi_d(E)$ and $\Phi_u(E)$ were calculated using the stepped electron detector measurements and averaged over an auroral precipitation event, usually considering a fairly wide spatial interval of 400–800 km along the satellite track. Logarithmic interpolation was used to find $\Phi_d(E)$ between the 16 energy step levels and logarithmic extrapolation employed to estimate the flux from 200 eV down to 100 eV and from 26 keV up to 30 keV. The downward flux applied to the top model level at 400 km was then adjusted in the 200–1000 eV range so that the modeled $\Phi_d(E)$ at satellite altitude matched the measured $\Phi_d(E)$. This adjustment was never greater than a 15% increase. Fluxes at satellite altitude for the two auroral events displayed in Figures 3*b* and 4*b* are plotted in Figures 6*a*, 6*b*. Comparison between measured and modeled upward fluxes is very good. This is quite encouraging as it indicates that the backscatter ratios and elastic cross sections are correct. Furthermore, it shows that no significant portion of the primary flux went unmeasured as the satellite flew through a structured, anisotropic event. When this occurs, it will show up as an unexplained increase in $\Phi_u(E)$; this was observed on only one of the orbits analyzed.

One potential difficulty with the two-stream method is that it can fail to conserve energy when applied to keV fluxes if the altitude and energy resolution is not adequate. To evaluate this problem, all energy output from the model—the sum of excitation, ionization, heating, and backscatter energies—is computed for each run and compared to that which was input. For insufficiently fine altitude grids, flux calculations start to become unstable near the peak deposition altitude and energy is "created". Even at the 2 km grid spacing used to overcome this, there is a 10% increase in output energy, mostly occurring below 120 km. This is below the region of interest for 6300 Å studies, and is thus only of concern when comparison is made to emissions emanating from low altitude such as the N_2^+ 1NG bands.

The two-stream code was compared to several other electron transport codes using the same atmospheric parameters and electron fluxes. Correspondence was fairly good for a variety of fluxes ranging from a soft 150 eV Maxwellian, to a hard 10 keV exponential flux. Models employed in the study were supplied by R. Link and M. H. Rees, and from the published multistream calculation of *Strickland et al.* [1976]. The results of these comparisons are not shown here but may be found in *Solomon* [1987]. The conclusions were that the two-stream method slightly overestimates (by about 10%) energy deposition at the peak emission altitude, but it is a sufficient method for calculation of fluxes in the 150250 km altitude range, which is the atmospheric region of interest for study of auroral O(^1D).

The semi-empirical mass spectrometer incoherent scatter (MSIS–83) model [*Hedin*, 1983] was used to obtain neutral densities. Despite its wide acceptance by the aeronomy community, there is still a great deal of doubt as to whether this model (or any other) gives a realistic portrait of composition, particularly of atomic oxygen densities, in auroral arcs. Because of increased turbulence and heating at the altitudes of major auroral energy deposition (100–150 km), it is assumed that transport occurs from lower thermosphere to upper, resulting in a lower proportion of light atomic species than would be found elsewhere. Neutral winds then redistribute this mix through the polar regions before diffusion can restore the equilibrium profile. Satellite measurements of individual species incorporated into MSIS should take this into account, but there is some doubt that the full structure in the vicinity of a discrete auroral event is predicted by a model that is based on global averaging.

To investigate this question, 120 auroral oval transits made by the AE–C satellite during its elliptical phase were analyzed. Rather than specify the auroral zone by geophysical coordi-

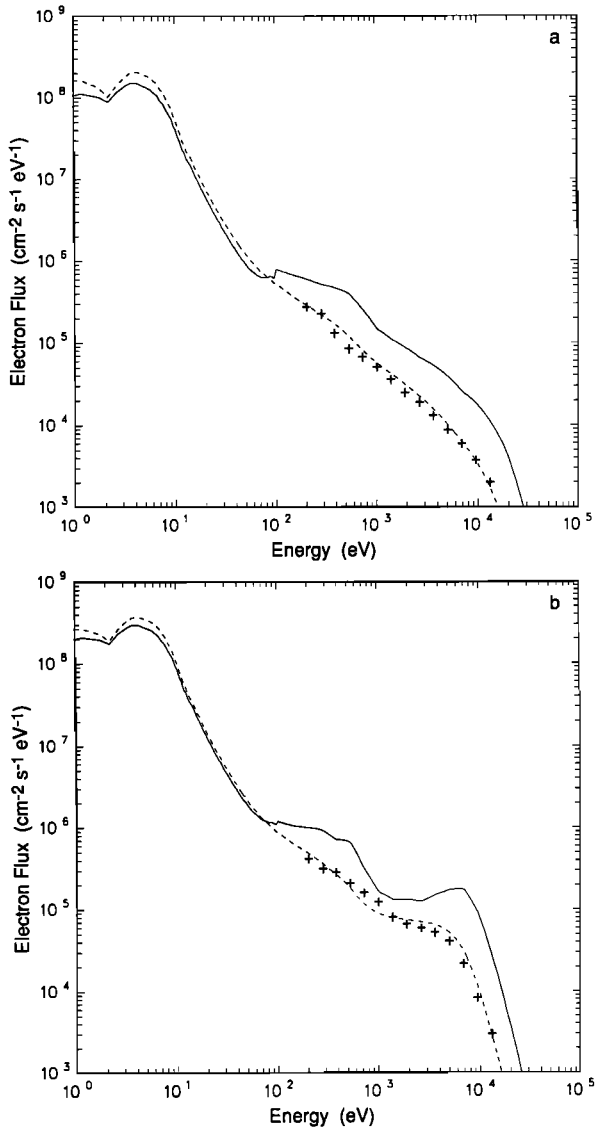

Fig 6. Hemispherical electron fluxes measured by LEE and modeled at the satellite altitude using the two-stream code. (*a*) AE–C orbit 5378 from 44890 to 44990 s UT. (*b*) AE–C orbit 6136 from 40650 to 40740 s UT. Solid line, modeled downward; dotted line, modeled upward; plus, measured upward.

nates, UA data from the LEE detectors were monitored to detect the presence of significant electron flux activity. The O and N_2 densities measured by the open source spectrometer (OSS) [*Nier et al.*, 1973] were taken from the UA database at these points. The ratios between measured densities and those predicted by the MSIS model for that geophysical location were then calculated. The overall nighttime average of the ratio O_{OSS}/O_{MSIS} was 0.9, a small but significant reduction of atomic oxygen compared to the model. Molecular nitrogen was conversely raised by a factor of about 1.1 over the MSIS values, indicating that a vertical transport mechanism may be responsible. Molecular oxygen was not measured on these orbits.

These results were only used for orbits where mass spectrometer measurements of neutral composition at the satellite altitude were not made. For most orbits analyzed here, OSS data were available from the UA files and were used to normalize the MSIS values. The average O and N_2 densities over the auroral event were divided by the MSIS prediction for that location, and the entire MSIS profile multiplied by that number. No attempt was made to adjust the O_2 distribution as that species has little effect on electron deposition at high altitude, but the O_2^+ profile was adjusted using densities measured by the Bennett ion mass spectrometer (BIMS) [*Brinton et al.*, 1973] as described below, to account for any deviations due to inadequate knowledge of O_2. Orbits for which composition data were unavailable had their O and N_2 profiles adjusted by 10% downward and upward, respectively. The electron density profile is also important as heating of the ambient electron gas competes with $O(^1D)$ excitation as a sink of low-energy secondary electrons. The transport code and chemical model were therefore run twice for each event, first with an assumed electron density profile, then again using the profile calculated in the first run as described below.

Electron, ion, and neutral temperatures were also measured by the cylindrical electrostatic probe (CEP) [*Brace et al.*, 1973], by the retarding potential analyzer (RPA) [*Hanson et al.*, 1973], and by the neutral atmosphere temperature experiment (NATE) [*Spencer et al.*, 1973], respectively. The electron temperature was treated by assuming an isothermal distribution equal to the measured value above 200 km and a linear decrease to 300 K at the turbopause. Most measured values were in the neighborhood of 2000 K. The ion and neutral temperatures were estimated by normalizing the MSIS temperature profile to RPA and NATE measurements. The neutral temperature was generally elevated by about 100 K above the MSIS prediction, the ion temperature usually another 100–300 K above that.

The computations described above yield electron impact excitation and ionization rates as a function of altitude; to calculate the contributions to excitation of the $O(^1D)$ metastable chemical reactions among atmospheric constituents must be considered. The model created for use with this data is a one-dimensional, steady state reaction scheme with no transport or diffusion effects. This is a considerable simplification of the actual situation, which may be justified by the following reasoning. The measured emission profile averaged over a discrete auroral precipitation event is the most accurate piece of information recovered from the photometer data analysis, it is best compared to a similarly averaged set of electron flux measurements. The history of the electron flux in that region is not known, so time dependent calculations yield no additional information. Also, the bulk motions of the upper atmosphere are not measured so addition of horizontal transport effects would be speculative; conditions outside the plane of the satellite orbit are likewise unknown so the transport contribution to changes in density of long-lived species is obscure. Vertical diffusion is important for distribution of electrons and atomic oxygen ions above 200 km, but a more accurate means of finding these parameters is to measure them at satellite altitude near 250 km. Diffusion of metastables such as $N(^2D)$ and $O(^1D)$ only becomes important above this altitude.

The chemical reactions and rate coefficients are tabulated in Appendix B. In addition to the excited and ionized species, neutral species are included in the model which participate in the chemistry but whose densities are not adjusted but rather assumed to remain constant—$O(^3P)$, O_2, N_2 and NO. The first three are determined as described above, the latter is taken from the model calculation of *Gérard and Rusch* [1979]. $N(^4S)$ is not considered here; its minor contribution to chemistry leading to $O(^1D)$ excitation is essentially similar to that of NO and so is contained in the uncertainty inherent in the adoption of an assumed profile for that species. $N(^2P)$ is also not specifically

considered as its density is so low; however, paths leading to $N(^2P)$ are included in $N(^2D)$ excitation so this species is implicitly contained in the $N(^2D)$ density. This simplification should be kept in mind when considering the estimation of $N(^2D)$ reaction branching ratios; some of the contributions may stem from $N(^2P)$.

The literature on reactions producing $O(^1D)$ is reviewed in the introduction. As indicated there, branching ratios for several of these reactions are ill-defined, controversial, or unknown. The values used in the model are summarized here due to their importance. The quantum yield for production of $O(^1D)$ by dissociative recombination of O_2^+ was taken as 1.2 [*Abreu et al.*, 1986]. $O(^1D)$ production from reaction of $N(^2D)$ with O_2 was assumed to be the upper limit value of 0.1 promulgated by *Link* [1983] and substantiated by *Langford et al.* [1986]. Reaction of $N(^2D)$ (with a possible contribution from $N(^2P)$) with O was treated as a free parameter and estimated to have an $O(^1D)$ quantum yield of 0.1. The rate coefficient for this reaction is a problem as laboratory measurements [*Davenport et al.*, 1976; *Iannuzzi and Kaufman*, 1980] find a rate three to four times faster than the aeronomically derived results [*Frederick and Rusch*, 1977; *Richards et al.*, 1981]. The Davenport et al. value of 1.8×10^{-12} was used here, although work in progress indicates that the rate may be an order of magnitude greater at thermospheric temperatures [*Jusinski and Slanger*, 1987]. A rate coefficient this large is difficult to reconcile with measurements of the 5200 Å emission. If true, it indicates serious misunderstanding of $N(^2D)$ sources or a problem with the $N(^4S$–$^2D)$ transition coefficient. Until this can be resolved, the Davenport et al. value is adopted as a compromise. The *Langford et al.* [1985, 1986] measurements were used to establish the fraction of $O(^1D)$ created when N^+ reacts with O_2 to give NO^+ and O at 0.7. The $O(^1D)$ yield for the reaction of $O^+(^2D)$ with O is not known; an arbitrary value of 0.5 was used in this study. Finally, there is a minor contribution to the $O(^1D)$ density from radiative cascade of $O(^1S)$ emitting a 5577 Å photon. It is not the objective of this study to solve the $O(^1S)$ problem, but an estimate must be made in order to include this source. Energy transfer from $N_2(A^3\Sigma_u^+)$ was considered to be the major source, using the *Piper et al.* [1981*a*] and *Piper* [1982] rates. Energy transfer from excited molecular oxygen was included [*Solheim and Llewellyn*, 1979] but arbitrarily attenuated by a factor of 10 so as to account for the combination of the A, A', and c states in one excitation category and because otherwise the modeled 5577/4278 Å ratio would be unrealistically high. Electron impact on atomic oxygen and dissociative recombination of O_2^+ were also included, using 0.1 as the $O(^1S)$ quantum yield from the latter [*Abreu et al.*, 1983].

Assuming a steady state, the system of partial differential equations resulting from the adopted reaction scheme reduces to a system of algebraic equations. The method used to find the solution to this system is a hybrid between analytic and iterative methodologies which exploits the energy hierarchy of the reactive species. Constraints arising from in situ measurements are also incorporated. First, an initial electron density profile is assumed, and the densities of all atomic ions are calculated by equating their production and loss rates. The O_2^+ density is then estimated, and the NO^+ and electron densities obtained by solving simultaneously the equations for charge neutrality and NO^+ at steady state equilibrium, resulting in

$$[e]^2(z) - q(z)\,[e](z) - p(z) = 0 \qquad (12)$$

where $q(z)$ is the sum of all ions other than NO^+ and $p(z)$ is the ratio of NO^+ production from all sources to the rate coefficient for dissociative recombination. Only one root of (12) is positive. This electron density profile is then adjusted to take into account the effect of diffusion and to force correspondence with that measured at the satellite altitude by RPA. Below 200 km, chemical equilibrium is assumed and no change is made; above this altitude the density is specified by linear interpolation between the modeled 200 km value and the measured one at satellite altitude near 250 km. Using this new electron profile, all ion densities including NO^+ are computed. $O^+(^4S)$ is adjusted above 200 km to preserve charge neutrality as it is the diffusing species. Then the quadratic expression for electron density is applied again, the profile readjusted, the ions computed and a few more iterations performed to assure convergence, which is rapid. Finally, the O_2^+ profile is normalized to the value measured by BIMS to account for uncertainties in the molecular oxygen density as described above. (BIMS ion composition measurements taken from the UA data base are adjusted upward by a factor of 1.27 on satellite AE–C, (2.35 on AE–E) by virtue of a statistical comparison between the sum of all ions from BIMS and the RPA total plasma density. See *Abreu et al.* [1983] and *Abreu et al.* [1986].) All other ions are adjusted proportionally to preserve charge neutrality; this is a very minor effect as O_2^+ is never the dominant ion.

With the ion chemistry determined, it is a simple matter to find the steady state equilibrium densities for each neutral excited species in turn, again working from higher energy to low. Figure 7 shows the results of these calculations for AE–C orbit 5378; electrons, all ground state ions, and the excited metastables $O(^1D)$ and $N(^2D)$ are displayed.

Comparison of Model to Observations

Contributions to the 6300 Å auroral volume emission rate profile are broken down into each component reaction and plotted for several orbits. All sources which reached a value greater than 1 photon cm^{-3} s^{-1} are plotted; thermal electron excitation of atomic oxygen, and energy transfer from $O^+(^2D)$ to $O(^3P)$ were below the lower limit plotted here. The largest contribution is from energetic electron impact on atomic

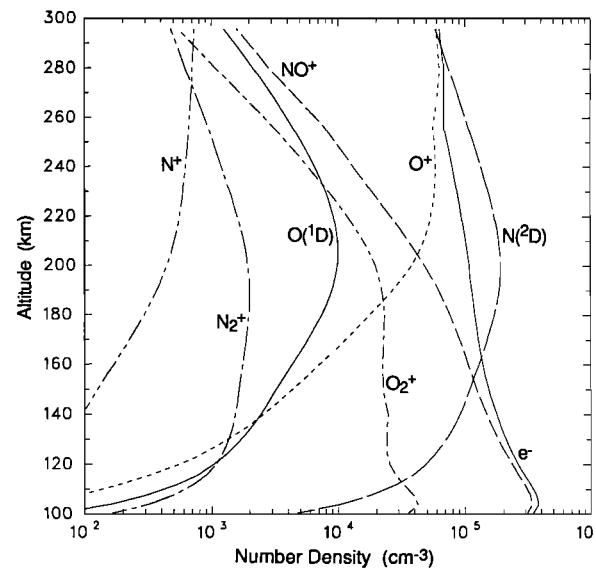

Fig. 7. Calculated densities for the auroral precipitation event from AE–C orbit 5378.

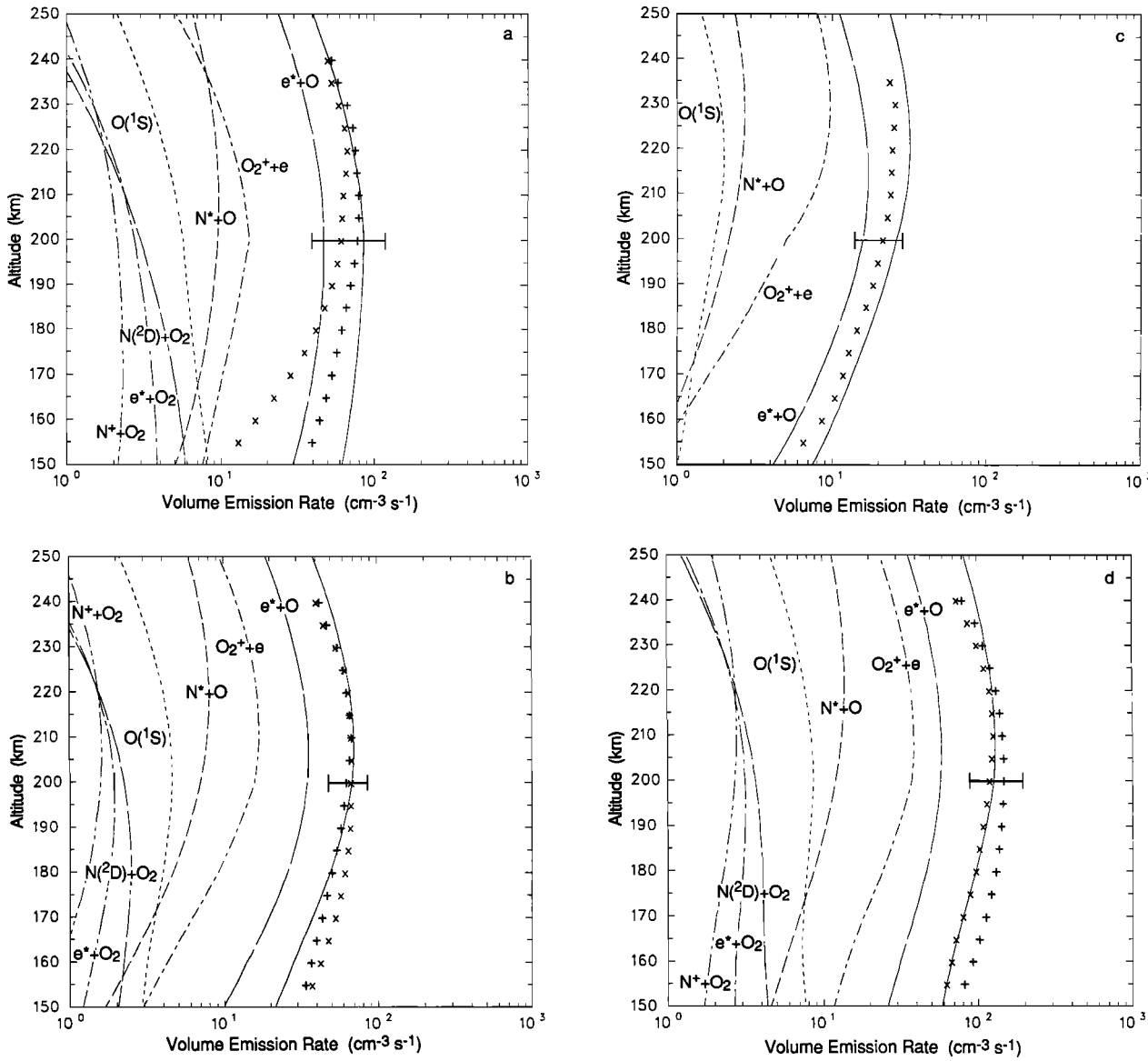

Fig. 8. Modeled and measured 6300 Å volume emission rates plotted as a function of altitude. (*a*) AE–C orbit 5376 from 34100 to 34190 s UT. (*b*) AE–C orbit 5378 from 44890 to 44990 s UT. (*c*) AE–C orbit 5631 from 15760 to 15860 s UT. (*d*) AE–C orbit 6136 from 40650 to 40740 s UT. Solid line, total modeled; broken line, e^*+O; dash-dot, $O_2^+ + e$; short dashes, N^*+O; long dashes, $N(^2D)+O_2$; dotted line, $O(^1S)$; long dash-dot, e^*+O_2; dash-dot-dot, $N^+ + O_2$; plus, measurement in forward direction; cross, measurement in backward direction. The error bar represents the estimated uncertainty in the measured profile.

oxygen. Another significant contribution comes from the dissociative recombination of O_2^+. Smaller amounts are predicted from quenching of excited atomic nitrogen, reaction of $N(^2D)$ with O_2, electron impact dissociation of O_2, and reaction of N^+ with O_2. Radiative cascade from $O(^1S)$ results in a fair amount of 6300 Å emission, particularly at low altitude, but there are great uncertainties in this calculation at the present time since this model makes only a rough initial attempt at solving accurately for the $O(^1S)$ density.

Volume emission rate profiles modeled using the methods described were compared to measurements made using the tomographic inversion for eight AE–C orbits. Altitude profiles were obtained by averaging several columns from the deduced emission rate function over an interval equal to the averaging interval for the electron fluxes, thus avoiding any problems due to inadequate horizontal resolution or difference in spatial scale. Figures 8*a*–8*d* contain a sample of the results. The error bar at 200 km represents the estimated uncertainty in the measured volume emission rate; the uncertainty is about 20% larger at 150 km but is comparable in magnitude throughout the 150–250 km region for this type of altitude profile [*Solomon et al.*, 1985]. Considering the experimental uncertainties correspondence between model and measurement ranges from fair to excellent. The volume emission rate at low altitude is overestimated by the model for orbit 5376 but underestimated for orbit 5378; orbit 5631 shows very good shape agreement although the magnitude of the model is a little high and orbit 6136 shows nearly perfect low altitude agreement for the forward viewing direction but not for the backward. Comparison of the forward and backward observations, where available, gives some idea of the temporal variation of the emission.

The model uncertainties have not been explicitly calculated

but are estimated to range from 30% for straightforward, empirically based calculations such as dissociative recombination of O_2^+ upward to 60% or more for reactions with ill-determined rates such as the $N(^2D)$ ones; in addition the calculation of $[N(^2D)]$ itself is complex and there are unresolved temporal and spatial effects on this long-lived metastable. The uncertainty for the e^*+O source would also be within 30% if the validity of the modeled secondary fluxes were accepted and the cross section considered well-defined; since there is dispute concerning these points, the uncertainty must be considered large. The shapes of the altitude profiles are the best indication of the relative importance of source reactions. The absolute scale of model and measurement may be difficult to pin down, but the altitude dependence of the emission and its changes with flux characteristics are indicative of the source mechanisms involved. Examination of the $N(^2D)+O_2$ profile in comparison with the measured profiles indicates that this reaction is probably not the major source of auroral $O(^1D)$. When the quantum yields from this reaction and from the N*+O quenching reaction are treated as free parameters, the best fit to the data is obtained when both equal approximately 0.1.

As an additional check, it is desirable to use a simpler measurement technique to compare model and measurement. By averaging nadir brightness measurements over an auroral event from the channel one 6300 Å filter and the channel two 4278 Å filter and taking their ratio, the effects of ground reflection cancel if it is assumed that the albedo is invariant over this spectral interval. There may be some temporal differences due to the longer lifetime of $O(^1D)$ compared to the promptly emitting N_2^+ 1NG bands, but at the peak of the emitting layer $O(^1D)$ lifetimes are only of the order of 20 s, and by averaging over a wide region where the electron flux appears relatively stable any such deviations should be slight. Model prediction of this ratio may then be compared to the measured one. This was done for eight auroral events, and the result plotted in Figure 9. The slope of a line fitted to the points is 0.8, indicating that slight problems still remain in the analysis. Most of this is probably due to two discrepancies, however. The first is described above—energy deposition is overestimated at the auroral peak by about 10%. This will effect the calculation of 4278 Å emission but not 6300 Å as quenching precludes significant red line radiation at low altitudes. The second is that there is often a small unexplained bump in measured 6300 Å profiles near 100 km; this could be due either to some contaminating emission such as from the OH Meinel, N_2^+ Meinel, or N_2 1PG bands, or it could be due to some source of $O(^1D)$ not considered here. If this accounts for an additional 10% of deviation, then the differences between model and measurement using this technique are explained, and agreement is satisfactory. Within the range of errors expected from these modeling efforts a 20% deviation is not significant at any rate.

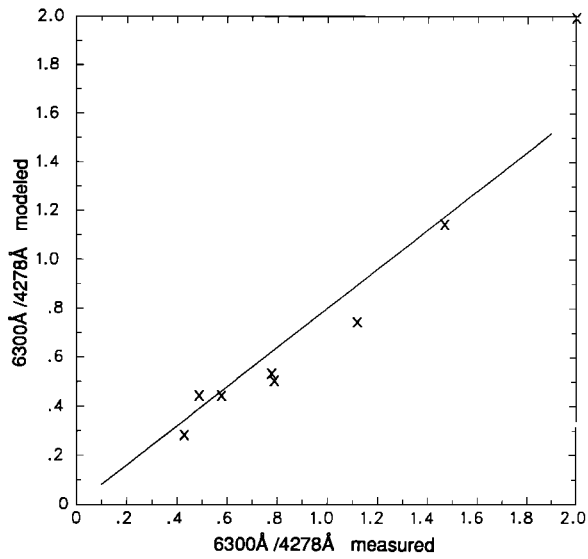

Fig. 9. Comparison of 6300/4278 Å brightness ratios. Vertical column brightness ratios viewed in the nadir direction from eight auroral passes are plotted against the modeled values. Slope of a linear fit is 0.8. Ground brightness was not subtracted.

The model was also applied to the March 21, 1974, coordinated satellite-rocket-ground experiment [*Rees et al.*, 1977; *Sharp et al.*, 1979]. The LEE measurements for this experiment pose a difficulty in that the measured spectrum for 0.2–26.0 keV only account for half of the energy deposition inferred from the N_2 1NG(0,0) 3914 Å column emission rate [*Sharp et al.*, 1979]. This may be resolved by assuming that half the energy is carried by electrons with energy greater than 26 keV, and extrapolating the measured primary flux to 40 keV [*Rees et al.*, 1977]. Following this procedure, and applying this spectrum to the model using an MSIS neutral atmosphere, results in good agreement between modeled ion and electron densities and those measured by the rocket flight above 100 km. The calculated N_2 2PG(0,0) 3371 Å emission in the 120–200 km region has a similar shape to the rocket measurement although 25–30% lower, but at the peak, 95 km, it was 70% higher. Comparison of the modeled secondary fluxes to those measured by the HARP instrument on the rocket is reasonable from 5 to 10 eV, but deteriorates rapidly with increasing energy until the model is about a factor of 10 lower at 100 eV, at 245 km altitude. Consequently, less 6300Å is predicted by the model than measured by the rocket, although the discrepancy is smaller than found by Sharp et al. At the peak of the emission profile, 225 km, the model is 40% lower than the measurement; at 150 km it is 65% lower. This argues for an increase in a low altitude source such as the $N(^2D)+O_2$ reaction proposed by *Rusch et al.* [1978], although this source would still be inadequate in the context of the present model owing to the higher rate adopted for quenching of $N(^2D)$ by O. It must be emphasized that the primary flux is not well known as it was measured for only 4 s by a spinning satellite and extrapolated above 26 keV. For the softer fluxes analyzed above such extrapolation is unimportant but when half the energy is carried by unmeasured electrons it may be questioned. Although ground based photometry showed that the aurora was stable throughout the experiment, an unexplained double peak in the electron density profile was observed. This could indicate that the primary flux had unusual spectral structure, which may be associated with spatial structure as well. Measurement of this type of flux with a spinning satellite is difficult. The discrepancy in the 3371 Å profile also indicates that the applied flux may be too hard.

Discussion

The primary conclusion drawn from this study of $O(^1D)$ in the aurora is that the "classical" production mechanisms, energetic electron impact excitation of atomic oxygen and dissociative recombination of O_2^+, account for the majority of the observed 6300 Å emission. This is hardly a new or radical finding, as it bring the situation back to about where it was 20 years ago. Considerable refinement has occurred, however, as the minor

sources were identified over time. A summary list is given below.

Production

$$e^* + O(^3P) \rightarrow e^* + O(^1D)$$
$$O_2^+ + e \rightarrow O + O(^1D)$$
$$N^* + O(^3P) \rightarrow N(^4S) + O(^1D)$$
$$O(^1S) \rightarrow O(^1D) + h\nu_{\lambda=5577\text{Å}}$$
$$N(^2D) + O_2 \rightarrow NO + O(^1D)$$
$$e^* + O_2 \rightarrow e^* + O + O(^1D)$$
$$N^+ + O_2 \rightarrow NO^+ + O(^1D)$$
$$e_t + O(^3P) \rightarrow e_t + O(^1D)$$
$$O^+(^2D) + O(^3P) \rightarrow O^+(^4S) + O(^1D)$$

Loss

$$O(^1D) + N_2 \rightarrow O(^3P) + N_2$$
$$O(^1D) + O_2 \rightarrow O(^3P) + O_2$$
$$O(^1D) + O(^3P) \rightarrow O(^3P) + O(^3P)$$
$$O(^1D) + e \rightarrow O(^3P) + e$$
$$O(^1D) \rightarrow O(^3P_2) + h\nu_{\lambda=6300\text{Å}}$$
$$O(^1D) \rightarrow O(^3P_1) + h\nu_{\lambda=6364\text{Å}}$$
$$O(^1D) \rightarrow O(^3P_0) + h\nu_{\lambda=6392\text{Å}}$$

Reaction of $N(^2D)$ with O_2 is included here with an $O(^1D)$ yield of 0.1 so scaling the source curves in *9a–9d* upward by a decade indicates the upper limit that may be generated by this mechanism using the adopted chemical scheme. A higher yield from this reaction cannot be ruled out on the basis of this work alone due to discrepancies in the profile at low altitude, uncertertainties in the chemistry of $N(^2D)$, and the contrary evidence of the March 21, 1974, coordination experiment. But the results presented here show no reason to dispute the *Langford et al.* [1986] laboratory findings, so if there is a missing source of $O(^1D)$ at low altitude which becomes important for very energetic fluxes, it remains unidentified.

In considering quenching by atomic oxygen, the quantity N*, the sum of excited atomic nitrogen in the ^2D and ^2P states, is used instead of considering $N(^2P)$ separately as its chemistry is not well known and explicit modeling would be speculative. The problem with the $N(^2D)$+O reaction as a source of $O(^1D)$ is that observations of 6300/5200 Å ratio variations in the polar cap show that the yield of $O(^1D)$ from $N(^2D)$+O is small, and the $O(^1D)$ nightglow chemistry does not admit an additional source from this mechanism. But this does not apply to reactions of $N(^2P)$. These observations indicate that some $O(^1D)$ may be produced by $N(^2P)$+O, although just how much remains obscure. Using the cross sections for electron impact dissociation of N_2 of *Zipf and McLaughlin* [1978], an upper limit on production of $O(^1D)$ equal to about 50% of the calculated e^*+O source at 200 km may be inferred for unit quantum yield. The yield is probably much smaller, however.

Radiative cascade from $O(^1S)$ is also important, particularly at low altitude. Thermal electron excitation of $O(^3P)$ is an important source when the electron temperature is greatly elevated, but not in the auroræ studied here. Electron impact dissociation of O_2 and reaction of N^+ with O_2 are very minor sources and energy transfer from $O^+(^2D)$ to $O(^3P)$ is insignificant. The conditions of this study specifies the limitations on the generality of these conclusions; they are: night, low solar activity, moderately energetic electron fluxes, and high magnetic latitude.

The conclusion that electron impact on atomic oxygen supplies the largest portion of auroral $O(^1D)$ hinges on the acceptance of the high rates of secondary electron production predicted by collisional models. It must be repeated that high fluxes at low energy are not always observed, and that other studies have concluded that electron impact produces little $O(^1D)$ in auroræ [e.g., *Rusch et al.*, 1978; *Sharp et al.*, 1983; *Rees and Roble*, 1986]. Also, the density of atomic oxygen in the aurora and in the thermosphere in general is another controversial subject [cf. *Torr and Sharp*, 1979; *McDade and Llewellyn*, 1984] which affects the calculation of $O(^1D)$ production. At the higher altitude of 6300 Å emission, the question of turbopause peak atomic oxygen density is not important. The auroral density question at higher altitudes has been partly surmounted by the use of measured densities to normalize the modeled profile whenever possible; this procedure has the most validity near the satellite orbit and its reliability diminishes with decreasing altitude. Use of in situ ion and electron density measurements also augments the validity of the modeled O_2^+ dissociative recombination source.

Loss rates of $O(^1D)$ are also crucial in determining the 6300 Å emission. Of those considered here, the one with the largest uncertainty is quenching by $O(^3P)$. This topic is discussed in *Abreu et al.* [1986], where it is concluded that if the consensus laboratory rate for quenching by N_2 and the *Fischer and Saha* [1983] transition coefficients are accepted as the best available determinations of these quantities, quenching by O as calculated by Yee et al. [1988] is required to explain the observed 6300 Å nightglow. *Link and Cogger* [1988] find from a reexamination of radar/optical observations that the lower *Kernahan and Pang* [1975] coefficients without atomic oxygen quenching are equally effective explaining the results as the Abreu et al. loss rates. The same is essentially true here—the altitude variation of the atomic oxygen loss rate is not so great and the proportion of loss attributable to this mechanism not so large that neglecting the $O(^1D)$+$O(^3P)$ reaction and using lower transition coefficients would greatly change the conclusions. However, there would be slightly more room for increased low-altitude production, such as from reaction of $N(^2D)$ with O_2, if this were the case.

Because of the discrepancies and uncertainties at lower altitude, this study cannot rule out a greather quantum yield of $O(^1D)$ from $N(^2D)$+O_2 than the nominal value of 0.1 adopted here. In addition, the $N(^2D)$ chemistry will be unclear until the question of the rate of quenching by O is settled. This rate is not only of importance to auroral chemistry but also to the odd nitrogen balance in general. If the results of *Jusinski and Slanger* [1987] prove correct, debate concerning the $N(^2D)$+O_2 reaction will become moot. This debate will not be resolved until a definitive laboratory study of this reaction is carried out. There have been some useful recent experiments [*Langford et al.*, 1986; *Rawlins*, 1986], but none specifically designed to measure the quantum yield of $O(^1D)$ from this reaction. In addition, the products and rate of the reaction of $N(^2P)$ with O need further investigation. New laboratory experiments and theoretical studies of these reactions of excited atomic nitrogen are indicated.

Appendix A: Electron Impact Cross Sections

All inelastic cross sections employed in the electron transport code were approximated with analytical fitting functions, using the *Jackman et al.* [1977] formula for ionization and secondary electron production and the *Green and Stolarski* [1972] equation for excitation. The Jackman et al. values were retained, with the exception of the linear coefficients for O which were adjusted to match the results of *Burnett and Rountree*

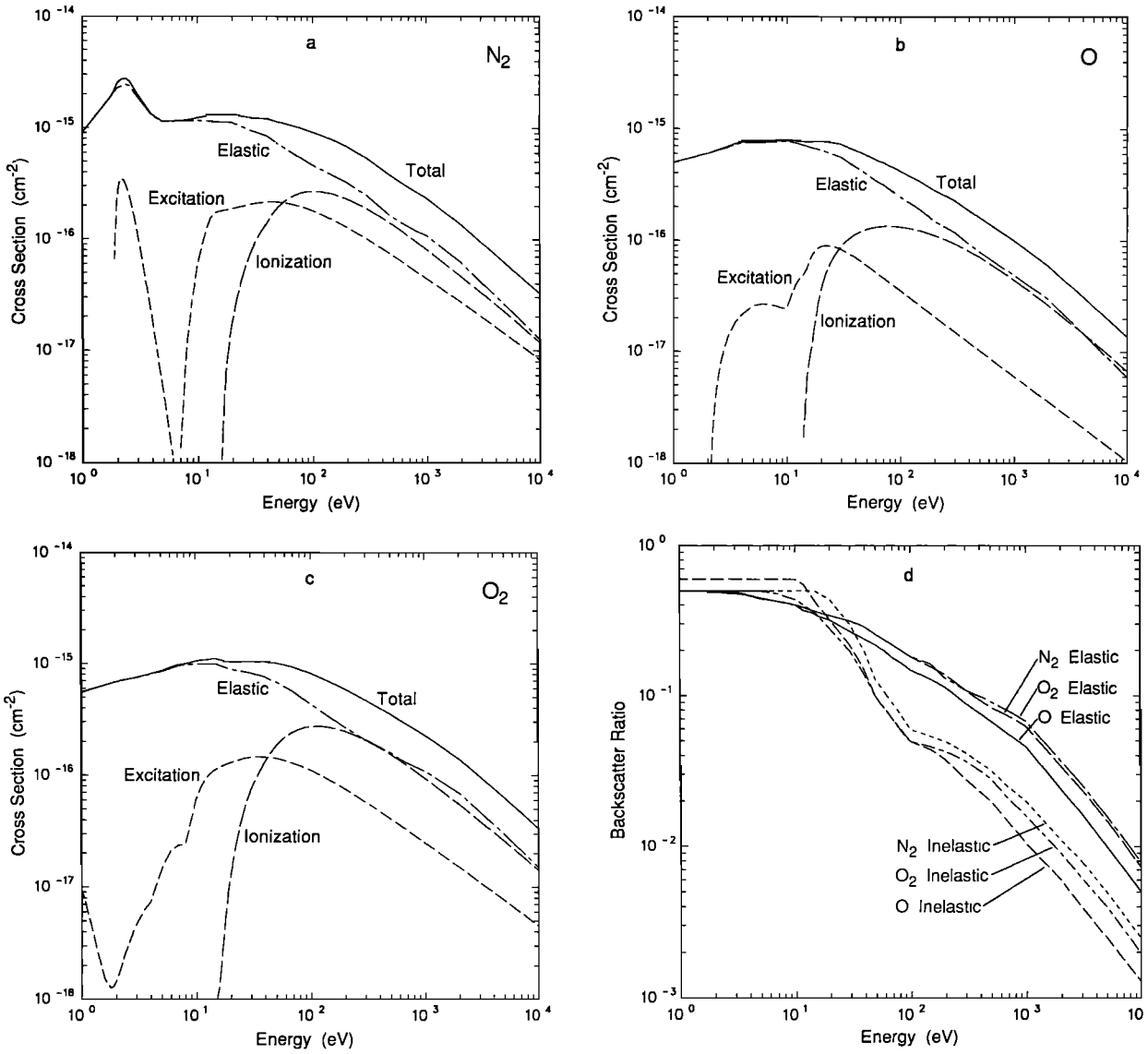

Fig. A1. Electron impact cross sections for (*a*) N_2, (*b*) O, (*c*) O_2, and (d) backscatter ratios for μ=0.577.

[1979] as suggested by *Link* [1982]. Many of the Green and Stolarski excitation cross sections were re-fit, however, to reflect subsequent measurements and revisions. For N_2, the sum of vibrational excitaion was taken from *Porter et al.* [1976], and the A, B, B', W, C, a, a', and w states were taken from *Cartwright et al.* [1977*b*] as revised by *Trajmar et al.* [1983]. This downward revision brings the total cross section closer to *Pritchford and Phelps* [1982] in the 10-30 eV region. The b' and sum of the $^1\Pi_u$ states were taken from *Zipf and McLaughlin* [1978] and for the sum of the Rydberg states the Green and Stolarski representation was retained but normalized downward so as to reproduce the *Zipf and McLaughlin* total dissociation cross section when added to the b' and $^1\Pi_u$ cross sections. For O, ^1D and ^1S were unchanged from the Green and Stolarski values (see introduction for a discussion of the O(^1D) cross section), $^5S^0$ and $3d^3D^0$ taken from *Zipf and Erdman* [1985], $^3S^0$ and $^3D^0$ from *Vaughn and Doering* [1987], the sum of the Δs=1 transitions unchanged, and the sum of the remaining Δs=0, Δl=0 and Δs=0, Δl=1 transitions taken from *Jackman et al.* [1977]. For O_2, the vibrational, a, and b cross sections used were the values of *Phelps* as cited by *Stamnes and Rees* [1983], the A, A', c, SRC, and 9.9 eV states taken from *Wakiya* [1978*a*,*b*], and the sum of the Rydberg states normalized downward from the Green and Stolarski curve [*Link*, 1982].

Elastic cross sections were interpolated from tabulated values, using a combination of theoretical results and experimental data. N_2 was drawn from the work of *Wedde and Strand* [1974], *Finn and Doering* [1975], *Kennerly* [1980], *Blaau et al.* [1980], *Dalba et al.* [1980], *Hoffman et al.* [1982], *Dubois and Rudd* [1976], *Shyn and Carignan* [1980], and *Srivastava et al.* [1976]. For O, the results of *Sunshine et al.* [1967], *Wedde and Strand* [1974], and *Blaha and Davis* [1975] were employed. O_2 was calculated using *Sunshine et al.* [1967], *Wedde and Strand* [1974], *Shyn and Sharp* [1982], *Salop and Nakano* [1970], and *Dalba et al.* [1980]. For all three species the screened Rutherford formula as applied by *Strickland et al.* [1976] was used above 1 keV. Much of the experimental data for molecular cross sections was obtained from the review of *Trajmar et al.* [1983], which is an invaluable source for molecules other than O_2 and N_2 as well.

The excitation, ionization, elastic, and total cross sections are plotted in Figures A1*a*, A1*b*, and A1*c* for N_2, O, and O_2 respectively. Figure A1*d* is a plot of the elastic and inelastic backscatter ratios employed for each species. They are valid

TABLE B1. Chemical Reactions and Rate Coefficients

Reaction	Rate Coefficient, $cm^3\ s^{-1}$	Reference
$O^+ + N_2 \rightarrow NO^+ + N$	$2.78\times10^{-13} \exp(2.07(T_f/300)^{-1} - 0.61(T_f/300)^{-2})$	*Chen et al.* [1978]
$O^+ + O_2 \rightarrow O_2^+ + O$	$3.33\times10^{-12} \exp(3.72(T_f/300)^{-1} - 1.87(T_f/300)^{-2})$	*Chen et al.* [1978]
$N_2^+ + O \rightarrow NO^+ + N$	$1.4\times10^{-10} (T_f/300)^{-.44}$	*McFarland et al.* [1974]
$N_2^+ + O_2 \rightarrow N_2 + O_2^+$	$5.0\times10^{-11} (T_f/300)^{-.8}$	*McFarland et al.* [1973]
$N(^2D) + O_2 \rightarrow NO + O$	6.0×10^{-12}	*Lin and Kaufman* [1971]
$N(^2D) + O \rightarrow N(^4S) + O$	1.8×10^{-12}	*Davenport et al.* [1976]
$N(^2D) + e \rightarrow N(^4S) + e$	$5.5\times10^{-10} (T_e/300)^{.5}$	*Frederick and Rusch* [1977]
$O(^1D) + N_2 \rightarrow O(^3P) + N_2$	$2.0\times10^{-11} \exp(107.8/T_n)$	*Streit et al.* [1976]
$O(^1D) + O_2 \rightarrow O(^3P) + O_2$	$2.9\times10^{-11} \exp(67.5/T_n)$	*Streit et al.* [1976]
$O(^1D) + e \rightarrow O(^3P) + e$	$8.1\times10^{-10} (T_e/300)^{.5}$	*Link* [1982]
$O(^1S) + O \rightarrow O(^3P) + O$	2.0×10^{-14}	*Slanger and Black* [1981]
$O^+(^2D) + N_2 \rightarrow O + N_2^+$	8.0×10^{-10}	*Johnsen and Biondi* [1980]
$O^+(^2D) + O_2 \rightarrow O + O_2^+$	7.0×10^{-10}	*Johnsen and Biondi* [1980]
$O^+(^2D) + e \rightarrow O^+(^4S) + e$	$6.6\times10^{-8} (T_e/300)^{-.5}$	*Henry et al.* [1969]
$O^+(^2D) + O \rightarrow O^+(^4S) + O$	1.0×10^{-11}	*Torr and Torr* [1980]
$O^+(^2P) + N_2 \rightarrow O + N_2^+$	4.8×10^{-10}	*Rusch et al.* [1977]
$O^+(^2P) + O_2 \rightarrow O + O_2^+$	4.8×10^{-10}	*Link* [1982]
$O^+(^2P) + e \rightarrow O^+(^2D, ^4S) + e$	$1.7\times10^{-7} (T_e/300)^{-.5}$	*Henry et al.* [1969]
$O^+(^2P) + O \rightarrow O^+(^4S) + O$	5.0×10^{-11}	*Rusch et al.* [1977]
$O_2^* + O \rightarrow O_2 + O$	$2.1\times10^{-11} \exp(-1136/T_n)$	*Solheim and Llewellyn* [1979]
$O_2^* + N_2 \rightarrow O_2 + N_2$	1.0×10^{-13}	*Solheim and Llewellyn* [1979]
$NO^+ + e \rightarrow N + O$	$2.3\times10^{-7} (T_e/300)^{-.5}$	*Mul and McGowen* [1979]
$N_2^+ + e \rightarrow N + N$	$3.5\times10^{-7} (T_e/300)^{-.5}$	*Mul and McGowen* [1979]
$O_2^+ + e \rightarrow O + O$	$1.9\times10^{-7} (T_e/300)^{-.5}$	*Mul and McGowen* [1979]
$N^+ + O_2 \rightarrow NO^+ + O, O_2^+ + N$	6.0×10^{-10}	*Langford et al.* [1985]
$N_2(A^3\Sigma_u^+) + O \rightarrow N_2 + O$	3.1×10^{-11} (av. v=1,2)	*Piper et al.* [1981*a*]
$O(^1D) + O \rightarrow O(^3P) + O$	8.0×10^{-12}	*Abreu et al.* [1986]
$O + e_t \rightarrow O(^1D) + e_t$	$2.6\times10^{-11} T_e^{.5} \exp(-22740/T_e)$	*Link* [1982]
$N_2(A^3\Sigma_u^+) + O_2 \rightarrow N_2 + O_2$	4.1×10^{-12}	*Piper et al.* [1981*b*]
$O_2^+ + NO \rightarrow O_2 + NO^+$	4.4×10^{-10}	*Lindenger and Ferguson* [1983]
$N(^2D) + NO \rightarrow N(^4S) + NO$	7.0×10^{-11}	*Fehsenfeld* [1977]
$N^+ + O \rightarrow N + O^+$	1.0×10^{-12}	*Torr* [1985]

only for an average pitch angle cosine of 0.577. Elastic backscatter was calculated by J. U. Kozyra (personal communication, 1986) using results from *Shyn et al.* [1972], *Shyn and Sharp* [1982], *Wedde and Strand* [1974], and *Stamnes* [1980; 1981]. Inelastic backscatter presents a problem as there are so few doubly differential measurements for energy loss that extend past ~135° scattering angle; in addition, the two-stream code treats all energy loss backscatter by a single species as one process, necessitating adoption of an average ratio. The approach taken was to use measurements where available [*Cartwright et al.*, 1977*a*; *Trajmar et al.*, 1983; *Shyn and Sharp*, 1986] and to assume for the remainder of processes that the backscatter ratio was 0.5 for forbidden transitions, identical to elastic scattering for allowed transitions, and zero for ionizing transitions. The average of all transitions, weighted by their relative contribution to the total inelastic cross section, was taken as a function of energy, resulting in the curves displayed in Figure A1*d*. These curves remain crude estimates, but electron transport calculations are comparitively insensitive to these parameters as pitch angle redistribution is dominated by elastic processes.

TABLE B2. Branching Ratios

Reaction	Yield	Reference
$O(^1S)$ from $O_2^+ + e$	0.1	*Abreu et al.* [1983]
$O(^1D)$ from $O_2^+ + e$	1.2	*Abreu et al.* [1986]
$N(^2D)$ from $NO^+ + e$	0.76	*Kley et al.* [1976]
$N(^2D)$ from $N_2^+ + e$	1.9	*Quéffelec et al.* [1985]
$N(^2D)$ from $N_2^+ + O$	1.0	*Frederick and Rusch* [1977]
$O(^1D)$ from $N(^2D) + O_2$	0.1	*Langford et al.* [1985]
$O^+(^2D)$ from $O^+(^2P) + e$	0.8	*Link* [1982]
N^+ from $N_2 + e^*$	0.16	*Richards and Torr* [1985]
$N(^2D) + N(^2P)$ from above	0.50	*Zipf et al.* [1980]
$NO^+ + O$ from $N^+ + O_2$	0.43	*Langford et al.* [1985]
$O(^1D)$ from above	0.7	*Langford et al.* [1985]
$O(^1S)$ from $N_2(A^3\Sigma_u^+) + O$	0.75	*Piper* [1982]
$O(^1S)$ from $O_2^* + O$	0.1	see text
$O(^1D)$ from $O^+(^2D) + O$	0.5	see text
$O(^1D)$ from $N^* + O$	0.1	see text

APPENDIX B: CHEMICAL REACTIONS

Table B1 lists the reactions used in the chemical model, their rate coefficients, and references for the rates employed. T_n, T_i, T_e, T_f are the neutral, ion, electron, and effective temperature, respectively. Branching ratios of importance to the model are given in Table B2, and the Einstein coefficients for spontaneous emission are specified in Table B3.

Table B3. Spontaneous Transition Coefficients

Transition	Coefficient, s^{-1}	Reference
$N(^4S–^2D)$, A_{5200}	1.07×10^{-5}	*Wiese et al.* [1966]
$O(^3P–^1D)$, A_{6300}	0.0071	*Fischer and Saha* [1983]
$O(^3P–^1D)$, A_{6364}	0.0022	*Fischer and Saha* [1983]
$O(^3P–^1S)$, A_{2972}	0.045	*Kernahan and Pang* [1975]
$O(^1D–^1S)$, A_{5577}	1.06	*Kernahan and Pang* [1975]
$O^+(^4S–^2D)$, A_{3726}	9.7×10^{-5}	*Kernahan and Pang* [1975]
$O^+(^4S–^2P)$, A_{2770}	0.0479	*Wiese et al.* [1966]
$O^+(^2D–^2P)$, A_{7320}	0.1712	*Wiese et al.* [1966]
$O_2(X–c)$, $A_{H\text{-}II}$	0.001	*Solheim and Llewellyn* [1979]
$N_2(X–A)$, $A_{V\text{-}K}$	0.77	*Shemansky* [1969]

Acknowledgments. The authors wish to thank Janet Kozyra, Andrew Nagy, Gordon Shepherd, and Jeng-Hwa Yee for consultations involving this study. John Doering and Robert Hoffman generously provided AE particle data. This work was supported by NASA grant NAGW-496 to the University of Michigan and by the National Center for Atmospheric Research.

The Editor thanks R. Link and P. Richards for their assistance in evaluating this paper.

REFERENCES

Abreu, V. J., S. C. Solomon, W. E. Sharp, and P. B. Hays, The dissociative recombination of O_2^+: The quantum yield of $O(^1S)$ and $O(^1D)$, *J. Geophys. Res.*, *88*, 4140, 1983.

Abreu, V. J., J. H. Yee, S. C. Solomon, and A. Dalgarno, The quenching rate of $O(^1D)$ by $O(^3P)$, *Planet. Space Sci.*, *11*, 1143, 1986.

Banks, P. M., C. R. Chappell, and A. F. Nagy, A new model for the interaction of auroral electrons with the thermosphere: Spectral degradation, backscatter, optical emission, and ionization, *J. Geophys. Res.*, *79*, 1459, 1974.

Banks, P. M., and A. F. Nagy, Concerning the influence of elastic scattering upon photoelectron transport and escape, *J. Geophys. Res.*, *75*, 1902, 1970.

Bates, D. R., *Mon. Not. R. Astron. Soc.*, *106*, 509, 1946.

Bates, D. R., Forbidden oxygen and nitrogen lines in the nightglow, *Planet. Space Sci.*, *26*, 897, 1978.

Bates, D. R., Airglow and auroras, in *Applied Atomic Collision Physics*, Academic, San Diego, Calif., 1982.

Blaauw, H. J., R. W. Wagenaar, D. H. Barends, and F. J. de Heer, *J. Phys. B*, *13*, 359, 1980.

Black, G., T. C. Slanger, G. A. St. John, and R. A. Young, Vacuum ultraviolet photolysis of N_2: Deactivation of $N(^2D)$, *J. Chem Phys.*, *51*, 116, 1969.

Blaha, M., and J. Davis, Elastic scattering of electrons by O and N_2 at intermediate energies, *Phys Rev. A*, *12*, 2319, 1975.

Brace, L. H., R. G. Theis, and A. Dalgarno, The cylindrical electrostatic probes for Atmosphere Explorer–C, –D, and –E, *Radio Sci.*, *8*, 341, 1973.

Brinton, H. C., L. R. Scott, M. W. Pharo, and J. T. Coulson, The Bennett ion mass spectrometer on Atmophere Explorer–C, –D, and –E, *Radio Sci.*, *8*, 323, 1973.

Brown, W. E., and W. R. Steiger, 6300 Å quantum efficiency of the recombination mechanism in the night-time *F* layer, *Planet. Space Sci.*, *20*, 11, 1972.

Burnett, T., and S. P. Rountree, Differential and total cross sections for electron-impact ionization of atomic oxygen, *Phys. Rev. A*, *20*, 1468, 1979.

Cartwright, D. C., A. Chutjian, S. Trajmar, and W. Williams, Electron impact excitation of the electronic states of N_2, I, Differrential cross sections at incident energies from 10 to 50 eV, *Phys. Rev. A*, *16*, 1013, 1977*a*.

Cartwright, D. C., A. Chutjian, S. Trajmar, and W. Williams, Electron impact excitation of the electronic states of N_2, II, Integral cross sections at incident energies from 10 to 50 eV, *Phys. Rev. A*, *16*, 1041, 1977*b*.

Chamberlain, J. W., *Physics of the Aurora and Airglow*, Academic, San Diego, Calif., 1961.

Chen, A., R. Johnsen, and M. A. Biondi, Measurements of the $O^+ + N_2$ and $O^+ + O_2$ reaction rates from 300 to 900 K, *J. Chem. Phys.*, *69*, 2688, 1978.

Cogger, L. L., J. C. G. Walker, J. W. Meriwether, Jr., and R. G. Burnside, F region airglow: are ground-based observations consistent with recent satellite results?, *J. Geophys. Res.*, *85*, 3013, 1980.

Cormack, A. M., Representation of a function by its line integrals, with some radiological applications *J. Appl. Phys.*, *34*, 2722, 1963.

Dalba, G., P. Fornasini, R. Grisenti, G. Ranieri, and A. Zecca, *J. Phys. B*, *13*, 4695, 1980.

Dalgarno, A., and G. Lejeune, The absorption of electrons in atomic oxygen, *Planet. Space Sci.*, *19*, 1653, 1971.

Dalgarno, A., and J. C. G. Walker, The red line of atomic oxygen in the day airglow, *J. Atmos. Sci.*, *21*, 463, 1964.

Davenport, J. E., T. G. Slanger, and G. Stewart, The quenching of $N(^2D)$ by $O(^3P)$, *J. Geophys. Res.*, *81*, 12, 1976.

Doering, J. P., and E. E. Gulcicek, Direct electron excitation cross sections for atomic oxygen at low energies, *Eos Trans. AGU*, *68*, 1392, 1987.

Doering, J. P., C. O. Bostrom, and J. C. Armstrong, The photoelectron spectrometer experiment on Atmosphere Explorer, *Radio Sci.*, *8*, 387, 1973.

Duboin, M. L., K. Lassen, and G. G. Shepherd, Observations of horizontal transport effects on high-latitude metastable $O(^1D)$, $N(^2D)$ auroral emissions, *Planet. Space Sci.*, *32*, 1407, 1984.

Dubois, R. D., and M. E. Rudd, *J. Phys. B*, *9*, 2657, 1976.

Evans, D. S., Precipitating electron fluxes formed by a magnetic field aligned potential difference, *J. Geophys. Res.*, *79*, 2853, 1974.

Fehsenfeld, F. C., The reaction of O_2^+ with atomic nitrogen, *Planet. Space Sci.*, *25*, 195, 1977.

Fischer, C. F., and H. P. Saha, Multiconfiguration Hartree-Fock results with Briet-Pauli corrections for forbidden transitions in the $2p^4$ configuration, *Phys. Rev. A*, *28*, 3169, 1983.

Fournier, J. P., and A. F. Nagy, The contribution of photoelectron impact excitation to the total intensity of the 6300 Å dayglow, *J. Atmos. Sci.*, *22*, 732, 1965.

Frank, L. A., and K. L. Ackerson, Observations of charged particle precipitation into the auroral zone, *J. Geophys. Res.*, *76*, 3612, 1971.

Frederick, J. E., and D. W. Rusch, On the chemistry of metastable atomic nitrogen in the *F* region deduced from simultaneous satellite measurements of the 5200 Å airglow and atmospheric composition, *J. Geophys. Res.*, *82*, 3509, 1977.

Finn, T. G., and J. P. Doering, Elastic scattering of 13 to 100 eV electrons from N_2, *J. Chem. Phys.*, *63*, 4399, 1975.

Fung, S. F., and R. A. Hoffman, On the spectrum of the auroral secondary electrons, *J Geophys. Res.*, *93*, 2715, 1988.

Garstang, R. H., Energy levels and transition probabilities in p^2 and p^4 configurations, *Mon. Not. R. Astron. Soc.*, *111*, 115, 1951.

Garstang, R. H., Transition probabilities in auroral lines, in *The Airglow and the Aurora*, edited by E. B. Armstrong and A. Dalgarno, Pergamon, New York, 1956.

Garstang, R. H., Transition probabilities for forbidden lines, in *Planetary Nebulae, IAU Symposium 34*, edited by D. E. Osterbrock and C. R. O'Dell, D. Reidel, Hingham, Mass., 1968.

Gérard, J. C., Metastable oxygen ion distribution and related optical emissions in aurora, *Ann. Geophys.*, *26*, 777, 1970.

Gérard, J. C., and O. E. Harang, Observation of $O(^1D)$ and $N(^2D)$ emission in the polar aurora, in *Physics and Chemistry of Upper Atmospheres*, edited by B. McCormac, D. Reidel, Hingham, Mass., 1973.

Gérard, J. C., and R. G. Roble, Transport of aurorally produced $N(^2D)$ by winds in the high latitude thermosphere, *Planet. Space Sci.*, *30*, 1091, 1982.

Gérard, J. C., and D. W. Rusch, The auroral ionosphere: Comparison of a time-dependent model with composition measurements, *J. Geophys. Res.*, *84*, 4335, 1979.

Green, A. E. S., and R. S. Stolarski, Analytic models of electron impact excitation cross sections, *J. Atmos. Terr. Phys.*, *34*, 1703, 1972.

Gulcicek, E. E., and J. P. Doering, Absolute differential and integral electron excitation cross sections of four forbidden transitions in atomic oxygen at 30 eV, *Eos Trans. AGU*, *67*, 1125, 1986.

Hanson, W. B., D. R. Zuccaro, C. R. Lippincott, and S. Sanatani, The retarding potential analyzer on Atmosphere Explorer, *Radio Sci.*, *8*, 309, 1973.

Hays, P. B., and C. D. Anger, Influence of ground scattering on satellite auroral observations, *Appl. Opt.*, *17*, 1898, 1978.

Hays, P. B., G. Carignan, B. C. Kennedy, G. G. Shepherd, and J. C. G. Walker, The visible airglow experiment on Atmosphere Explorer, *Radio Sci.*, *8*, 369, 1973.

Hays, P. B., D. W. Rusch, R. G. Roble, and J. C. G. Walker, The OI (6300 Å) airglow, *Rev. Geophys.*, *16*, 225, 1978.

Hedin, A. E., A revised thermospheric model based on mass spectrometer and incoherent scatter data: MSIS–83, *J. Geophys. Res.*, *88*, 10,170, 1983.

Henry, R. J. W., P. G. Burke, and A. L. Sinfailam, Scattering of electrons by C, N, O, N^+, O^+, and O^{++}, *Phys. Rev.*, *178*, 218, 1969.

Hernandez, G., Determination of the quenching of $O(^1D)$ by molecular nitrogen using the ionosphere modification experiment, *J. Geophys. Res.*, *77*, 3625, 1972.

Hoffman, K. R., M. S. Dababneh, H. F. Hsieh, W. E. Kauppila, V. Pol, J. H. Smart, and T. S. Stein, Total cross section measurements for positrons and electrons colliding with H_2, O_2, and CO_2, *Phys Rev. A*, *25*, 1393, 1982.

Hoffman, R. A., J. L. Burch, R. W. Janetzke, J. F. McChesney, and S. H. Way, Low-energy electron experiment for Atmosphere Explorer–C and –D, *Radio Sci.*, *8*, 393, 1973.

Hunten, D. M., and M. B. McElroy, Quenching of metastable states of atomic and molecular oxygen and nitrogen, *Rev. Geophys.*, *4*, 303, 1966.

Iannuzzi, M. P., and F. Kaufman, Rates of some reactions of N (^2D and ^2P) near 300 K, *J. Chem. Phys.*, *73*, 4701, 1980.

Jackman, C. H., R. H. Garvey, and A. E. S. Green, Electron impact on atmospheric gases, I, Updated cross sections, J. Geophys. Res., *82*, 5081, 1977.

Johnsen, R., and M. A. Biondi, Laboratory measurements of the $O^+(^2D)$ + N_2 and $O^+(^2D)$ + O_2 reaction rate coefficients and their ionospheric implications, *Geophys. Res. Lett.*, *7*, 401, 1980.

Jusinski, L. E., and T. G. Slanger, Determination of rate coefficient for quenching of $N(^2D)$ by $O(^3P)$, *Eos Trans. AGU*, *68*, 1388, 1987.

Kasting, J. F., and P. B. Hays, A comparison between N_2^+ 4278 Å emission and electron flux in the auroral zone, *J. Geophys. Res.*, *82*, 3319, 1977.

Kennealy, J. P., F. P. delGreco, G. E. Caledonia, and B. D. Green, Nitric oxide chemiexcitation occurring in the reaction between metastable nitrogen atoms and oxygen molecules, *J. Chem. Phys.*, *69*, 1574, 1978.

Kennerly, R. E., Absolute total electron scattering cross sections for N_2 between 0.5 and 50 eV, *Phys. Rev. A*, *21*, 1876, 1980.

Kernahan, J. H., and H. L. Pang, Experimental determination of absolute *A* coefficients for 'forbidden' atomic oxygen lines, *Can. J. Phys.*, *53*, 455, 1975.

Kley, D., G. M. Lawrence, and E. J. Stone, The yield of $N(^2D)$ atoms in the dissociative recombination of NO^+, *J. Chem. Phys.*, *66*, 4157, 1976.

Kozyra, J. U., Observational and theoretical investigations of stable auroral red arcs and their magnetospheric energy source, Ph.D. thesis, University of Mich., Ann Arbor, 1985.

Langford, A. O., V. M. Bierbaum, and S. R. Leone, Auroral implications of recent measurement on $O(^1S)$ and $O(^1D)$ formation in the reaction of N^+ with O_2, *Planet. Space Sci.*, *33*, 1225, 1985.

Langford, A. O., V. M. Bierbaum, and S. R. Leone, Branching ratios for electronically excited oxygen atoms formed in the reactions of N^+ with O_2 at 300 K, *J. Chem. Phys.*, *84*, 2158, 1986.

Lin, C. L., and F. Kaufman, Reactions of metastable nitrogen atoms, *J. Chem. Phys.*, *66*, 435, 1971.

Lindinger, W., and E. Ferguson, Laboratory investigation of the ionospheric $O_2^+(X^2\Pi,v=0)$ reaction with NO, *Planet. Space Sci.*, *31*, 1181, 1983.

Link, R., Dayside magnetospheric cleft auroral processes, Ph.D. thesis, York Univ., Toronto, Canada, 1982.

Link, R., A rocket observation of the 6300Å/5200Å intensity ratio in the dayside aurora: implications for the production of $O(^1D)$ via the reaction $N(^2D)+O_2 \rightarrow NO+O(^1D)$, *Geophys. Res. Lett.*, *10*, 225, 1983.

Link, R., and L. L. Cogger, A reexamination of the OI 6300 Å nightglow, *J. Geophys. Res.*, in press, 1988.

Link, R., J. C. McConnell, and G. G. Shepherd, A self-consistent evaluation of the rate constants for the production of the OI 6300 Å airglow, *Planet. Space Sci.*, *29*, 589, 1981.

Link, R., J. C. McConnell, and G. G. Shepherd, An analysis of the spatial distribution of dayside cleft optical emissions, *J. Geophys. Res.*, *88*, 10,145, 1983.

Mahadevan, P., and F. E. Roach, Mechanism for the auroral emission of OI (6300Å), *Nature*, *220*, 150, 1968.

McDade, I. C., and E. J. Llewellyn, Atomic oxygen concentrations in the auroral ionosphere, *Geophys. Res. Lett.*, *11*, 247, 1984.

McDade, I. C., and E. J. Llewellyn, A rocket measurement of the $O_2(b^1\Sigma_g^+-X^3\Sigma_g^-)(0,0)$ atmospheric band in a pulsating aurora, *Can. J. Phys.*, *63*, 1322, 1985.

McFarland, M., D. L. Albritton, F. C. Fehsenfeld, E. E. Ferguson, and A. L. Schmeltekopf, Flow-drift technique for ion mobility and ion-molecule reaction constant measurements, 2, Positive ion reactions of N^+, O^+, and N_2^+ with O_2 and O^+ with N_2 from thermal to approximately 2 eV, *J. Chem. Phys.*, *59*, 6620, 1973.

McFarland, M., D. L. Albritton, F. C. Fehsenfeld, E. E. Ferguson, and A. L. Schmeltekopf, Energy dependence and branching ratio of the N_2^+ and O reaction, *J. Geophys. Res.*, *79*, 2925, 1974.

Mul, P. M., and J. W. McGowan, Merged electron-ion beam experiments, III, Temperature dependence of dissociative recombination for atmospheric ions NO^+, O_2^+, and N_2^+, *J. Phys. B*, *12*, 1591, 1979.

Nagy, A. F., and P. M. Banks, Photoelectron fluxes in the ionosphere, *J. Geophys. Res.*, *75*, 6260, 1970.

Nier, A. O., W. E. Potter, D. R. Hickman, and K. Mauersberger, The open-source neutral-mass spectrometer on Atmosphere Explorer–C, *Radio Sci.*, *8*, 271, 1973.

Noxon, J. F., and A. E. Johanson, Effect of magnetically conjugate photoelectrons on OI (6300 Å), *Planet. Space Sci.*, *18*, 1367, 1970.

Olson, R. E., and F. T. Smith, Collision spectroscopy in diatomic systems, project PYU-1848, SRI Int., Menlo Park, Calif., 1974.

Opal, C. B., W. K. Peterson, and E. C. Beaty, Measurements of secondary-electron spectra produced by electron impact ionization of a number of simple gases, *J. Chem. Phys.*, *55*, 4100, 1971.

Papadopoulos, K., and T. Coffey, Nonthermal features of the auroral plasma due to precipitating electrons, *J. Geophys. Res.*, *79*, 674, 1974.

Piper, L. G., The excitation of $O(^1S)$ in the reaction between $N_2(A^3\Sigma_u^+)$ and $O(^3P)$, *J. Chem. Phys.*, *77*, 2373, 1982.

Piper, L. G., G. E. Caledonia, and J. P. Kennealy, Rate constants for deactivation of $N_2(A^3\Sigma_u^+,v'=0,1)$ by O, *J. Chem. Phys.*, *75*, 2847, 1981*a*.

Piper, L. G., G. E. Caledonia, and J. P. Kennealy, Rate constants for deactivation of $N_2(A^3\Sigma_u^+,v'=0,1)$ by O_2, *J. Chem. Phys.*, *75*, 2888, 1981*b*.

Porter, H. S., C. H. Jackman, and A. E. S. Green, Efficiencies for production of atomic nitrogen and oxygen by relativistic proton impact in air, *J. Chem. Phys.*, *65*, 154, 1976.

Pritchford, L. C., and A. V. Phelps, Comparative calculations of electron-swarm properties in N_2 at moderate *E/N* values, *Phys. Rev. A*, *25*, 540, 1982.

Quéffelec, J. L., B. R. Rowe, M. Morlais, J. C. Gomet, and F. Valée, The dissociative recombination of $N_2^+(v=0,1)$ as a source of metastable atoms in planetary atmospheres, *Planet. Space Sci.*, *33*, 263, 1985.

Rawlins, W. T., Rovibrational excitation of NO in the reaction of O_2 with metastable nitrogen, *Eos Trans. AGU*, *67*, 1125, 1986.

Rees, M. H., and R. A. Jones, Time dependent studies of the aurora, II, Spectroscopic morphology, *Planet. Space Sci.*, *21*, 1213, 1973.

Rees, M. H., and D. Luckey, Auroral emission energy derived from ratios of spectroscopic emissions, 1, Model computations, *J. Geophys. Res.*, *79*, 5181, 1974.

Rees, M. H., and R. G. Roble, Observations and theory of the formation of stable auroral red arcs, *Rev. Geophys.*, *13*, 201, 1975.

Rees, M. H., and R. G. Roble, Excitation of $O(^1D)$ atoms in auroræ and emission of the [OI] 6300 Å line, *Can. J. Phys.*, *64*, 1608, 1986.

Rees, M. H., J. C. G. Walker, and A. Dalgarno, Auroral excitation of the forbidden lines of atomic oxygen, *Planet. Space Sci.*, *15*, 1097, 1967.

Rees, M. H., A. I. Stewart, W. E. Sharp, P. B. Hays, R. A. Hoffman, L. H. Brace, J. P. Doering, and W. K. Peterson, Coordinated rocket and satellite measurements of an auroral event, 1, Satellite observations and analysis, *J. Geophys. Res.*, *82*, 2250, 1977.

Rees, M. H., B. A. Emery, R. G. Roble, and K. Stamnes, Neutral and ion gas heating by auroral electron precipitation, *J. Geophys. Res.*, *88*, 6289, 1983.

Richards, P. G., and D. G. Torr, On the production of N^+ by energetic electrons, *J. Geophys. Res.*, *90*, 9917, 1985.

Richards, P. G., D. G. Torr, and M. R. Torr, Photodissociation of N_2: A significant source of thermospheric atomic nitrogen, *J. Geophys. Res.*, *86*, 1495, 1981.

Roble, R. G., E. C. Ridley, and R. E. Dickinson, On the global mean structure of the thermosphere, *J. Geophys. Res.*, *92*, 8745, 1987.

Rusch, D. W., W. E. Sharp, and P. B. Hays, Twilight airglow, 3, OI 6300 Å radiation, *J. Geophys. Res.*, *80*, 1832, 1975.

Rusch, D. W., D. G. Torr, P. B. Hays, and J. C. G. Walker, The OII (7319–7320 Å) dayglow, *J. Geophys. Res.*, *82*, 719, 1977.

Rusch, D. W., J. C. Gérard, and W. E. Sharp, The reaction of $N(^2D)$ with O_2 as a source of $O(^1D)$ atoms in auroræ, *Geophys. Res. Lett.*, *5*, 1043, 1978.

Salop, A., and H. H. Nakano, Total electron scattering cross sections in O_2 and N_2, *Phys. Rev. A*, *2*, 127, 1970.

Schunk, R. W., and P. B. Hays, Photoelectron energy losses to thermal electrons, *Planet. Space Sci.*, *19*, 113, 1971.

Sharp, W. E., and P. B. Hays, Low-energy auroral electrons, *J. Geophys. Res.*, *79*, 4319, 1974.

Sharp, W. E., D. W. Rusch, and P. B. Hays, Dissociative recombination source of OI (^1D) atoms, *J. Geophys. Res.*, *80*, 2876, 1975.

Sharp, W. E., M. H. Rees, and A. E. Stewart, Coordinated rocket and satellite measurements of an auroral event, 2, The rocket observations and analysis, *J. Geophys. Res.*, *84*, 1977, 1979.

Sharp, W. E., D. Ortland, and R. Cageao, Conceming sources of $O(^1D)$ in aurora: Electron impact and dissociative recombination, *J. Geophys. Res.*, *88*, 3229, 1983.

Shemansky, D. E., N_2 Vegard-Kaplan system in absorption, *J. Chem. Phys.*, *51*, 689, 1969.

Shepherd, G. G., Dayside cleft aurora and its ionospheric effects, *Revs. Geophys. Space Phys.*, *17*, 2017, 1979.

Shyn, T. W., and G. R. Carignan, Angular distribution of electrons elastically scattered from gases: 1.5–400 eV on N_2, II, *Phys. Rev. A*, *22*, 923, 1980.

Shyn, T. W., and W. E. Sharp, Angular distribution of electrons elastically scattered from O_2: 2.0–200 eV impact energy, *Phys. Rev. A*, *26*, 1369, 1982.

Shyn, T. W., and W. E. Sharp, Differential excitation cross section of atomic oxygen by electron impact: (^3P–^1D transition), *J. Geophys. Res.*, *91*, 1691, 1986.

Shyn, T. W., R. S. Stolarski, and G. R. Carignan, Angular distribution of electrons elastically scattered from N_2, *Phys. Rev. A*, *6*, 1002, 1972.

Slanger, T. G., and G. Black, Quenching of $O(^1S)$ by $O(a^1\Delta_g)$, *Geophys. Res. Lett.*, *8*, 535, 1981.

Solheim, B. H., and E. J. Llewellyn, An indirect mechanism for the production of $O(^1S)$ in the aurora, *Planet. Space Sci.*, *27*, 473, 1979.

Solomon, S. C., Tomographic inversion of auroral emissions, Ph.D. thesis, Univ. of Mich., Ann Arbor, 1987.

Solomon, S. C., P. B. Hays, and V. J. Abreu, Tomographic inversion of satellite photometry, *Appl. Opt.*, *23*, 3409, 1984.

Solomon, S. C., P. B. Hays, and V. J. Abreu, Tomographic inversion of satellite photometry, II, *Appl. Opt.*, *24*, 4134, 1985.

Spencer, N. W., H. B. Niemann, and G. R. Carignan, The neutral atmosphere temperature instrument, *Radio Sci.*, *8*, 284, 1973.

Srivastava, S. K., A. Chutjian, and S. Trajmar, Absolute elastic differential electron scattering cross sections in the intermediate energy region, II, N_2, *J. Chem. Phys.*, *64*, 1340, 1976.

Stamnes, K., Analytic approach to auroral electron transport and energy degradation, *Planet. Space Sci.*, *28*, 427, 1980.

Stamnes, K., On the two-stream approach to electron transport and thermalization, *J. Geophys. Res.*, *86*, 2405, 1981.

Stamnes, K., and M. H. Rees, Inelastic scattering effects on photoelectron spectra and ionospheric electron temperature, *J. Geophys. Res.*, *88*, 6301, 1983.

Stasiewicz, K., On the origin of the auroral inverted-V electron spectra, *Planet. Space Sci.*, *32*, 379, 1984.

St. Maurice, J. P., and D. G. Torr, Nonthermal rate coefficients in the ionosphere: The reactions of O_2^+ with N_2, O_2, and NO, *J. Geophys. Res.*, *83*, 969, 1978.

Streit, G. E., J. H. Carleton, A. L. Schmeltekopf, J. A. Davidson, and H. I. Schiff, Temperature dependence of $O(^1D)$ rate constants for reactions with O_2, N_2, CO_2, O_3, and H_2O, *J. Chem. Phys.*, *65*, 4761, 1976.

Strickland, D. J., D. L. Book, T. P. Coffey, and J. A. Fedder, Transport equation techniques for the deposition of auroral electrons, *J. Geophys. Res.*, *81*, 2755, 1976.

Sunshine, G., B. B. Aubrey, and B. Bederson, Absolute measurements of total cross sections for the scattering of low-energy electrons by atomic and molecular oxygen, *Phys. Rev.*, *154*, 1, 1967.

Swartz, W. E., Optimization of energetic electron energy degradation calculations, *J. Geophys. Res.*, *90*, 6587, 1985.

Swartz, W. E., J. S. Nesbet, and A. E. S. Green, Analytical expression for the energy transfer rate from photoelectrons to thermal electrons, *J. Geophys. Res.*, *76*, 8425, 1971.

Thomas, L. D., and R. K. Nesbet, Low electron scattering by atomic oxygen, *Phys. Rev. A*, *11*, 170, 1976.

Torr, D. G., The photochemistry of the upper atmosphere, in *The Photochemistry of Atmospheres*, Academic, San Diego, Calif., 1985.

Torr, D. G., and W. E. Sharp, The concentratioin of atomic oxygen in the auroral lower thermosphere, *Geophys. Res. Lett.*, *6*, 860, 1979.

Torr, D. G., and M. R. Torr, Determination of the thermal rate coefficient, products, and branching ratios for the reaction of $O^+(^2D)$ with N_2, *J. Geophys. Res.*, *85*, 783, 1980.

Torr, D. G., P. G. Richards, and M. R. Torr, Destruction of $N(^2D)$ by O_2: A major source of 6300 Å dayglow emission, *Geophys. Res. Lett.*, *7*, 410, 1980.

Torr, D. G., P. G. Richards, M. R. Torr, and V. J. Abreu, Further quantification of the sources and sinks of thermospheric $O(^1D)$ atoms, *Planet. Space Sci.*, *29*, 595, 1981.

Torr, M. R., The NII 2143 Å dayglow from Spacelab 1, *J. Geophys. Res.*, *90*, 6679, 1985.

Torr, M. R., and D. G. Torr, The dissociative recombination of O_2^+ in the ionosphere, *Planet. Space Sci.*, *29*, 999, 1981.

Torr, M. R., and D. G. Torr, The role of metastable species in the thermosphere, *Rev. Geophys.*, *20*, 91, 1982.

Trajmar, S., D. F. Register, and A. Chutjian, Electron scattering by molecules II. Experimental methods and data, *Phys. Reports*, *97*, 219, 1983.

Vaughan, S. O., and J. P. Doering, Absolute experimental differential and integral electron excitation cross sections for atomic oxygen, 3, The ($^3P^3$–D^0) transition (989 Å) from 20 to 200 eV with improved values for the ($^3P^3$–S^0) transition (1304 Å), *J. Geophys. Res.*, *92*, 7749, 1987.

Vo Ky Lan, N. Feautrier, M. Le Doumeuf, and H. Van Regemorter, Cross section calculations for electron-oxygen scattering using the polarized orbital close coupling theory, *J. Phys. B*, *5*, 1506, 1972.

Wakiya, K., Differential and integral cross sections for the electron impact excitation of O_2, I, Optically allowed transitions from the ground state, *J. Phys. B*, *11*, 3913, 1978*a*.

Wakiya, K., Differential and integral cross sections for the electron impact excitation of O_2, II, Optically forbidden transitions from the ground state, *J. Phys. B*, *11*, 3931, 1978*b*.

Wallace, L., and M. B. McElroy, The visual dayglow, *Planet. Space Sci.*, *14*, 677, 1966.

Walls, F. G., and G. H. Dunn, Measurement of total cross sections for electron recombination with NO^+ and O_2^+ using storage techniques, *J. Geophys. Res.*, *79*, 1911, 1974.

Wedde, T., and T. G. Strand, Scattering cross sections for 40 eV to 1 keV electrons colliding elastically with nitrogen and oxygen, *J. Phys. B*, *7*, 1091, 1974.

Weill, G. M., NI(^4S–^2D) radiation in the night airglow and low latitude aurora, in *Atmospheric Emissions*, edited by B. M. McCormac and A. Omholt, Van Nostrand Reinhold, New York, 1969.

Wickwar, V. B., and W. Kofman, Dayside red auroras at very high latitudes: The importance of thermal excitation, *Geophys. Res. Lett.*, *11*, 923, 1984.

Wiese, W. L., M. W. Smith, and B. M. Glennon, Atomic transition probabilities, vol. 1, *Natl. Stand. Ref. Data Ser.—U. S. Nat. Bur. Stand.*, *4*, 1966.

Yee, J. H., S. L. Guberman, and A. Dalgarno, *Geophys. Res. Lett.*, submitted, 1988.

Zipf, E. C., The dissociative recombination of O_2^+ ions into specifically identified final atomic states, *Bull. Am. Phys. Soc.*, *15*, 418, 1970.

Zipf, E. C., and P. W. Erdman, Electron impact excitation of atomic oxygen: revised cross sections, *J. Geophys. Res.*, *90*, 11,087, 1985.

Zipf, E. C., and W. G. Fastie, An observation of the day airglow emission at 6300 Å, *J. Geophys. Res.*, *68*, 6208, 1963.

Zipf, E. C., and R. W. McLaughlin, On the dissociation of nitrogen by electron impact and by E.U.V. photo-absorption, *Planet. Space Sci.*, *26*, 449, 1978.

Zipf, E. C., P. S. Espy, and C. F. Boyle, The excitation and collisional deactivation of metastable $N(^2P)$ atoms in auroras, *J. Geophys. Res.*, *85*, 687, 1980.

V. J. Abreu and P. B. Hays, Space Physics Research Laboratory, University of Michigan, Ann Arbor, MI 48109.

S. C. Solomon, National Center for Atmospheric Research, Boulder, CO 80307.

(Received August 13, 1987;
revised March 21, 1988;
accepted May 2, 1988.)